Vortices in s-Wave Superconductors

A Numerical Study of the Bogoliubov-de Gennes Equations

Written by *Cecilie Hermansen*
June 13, 2018

Supervised by
Brian Møller Andersen

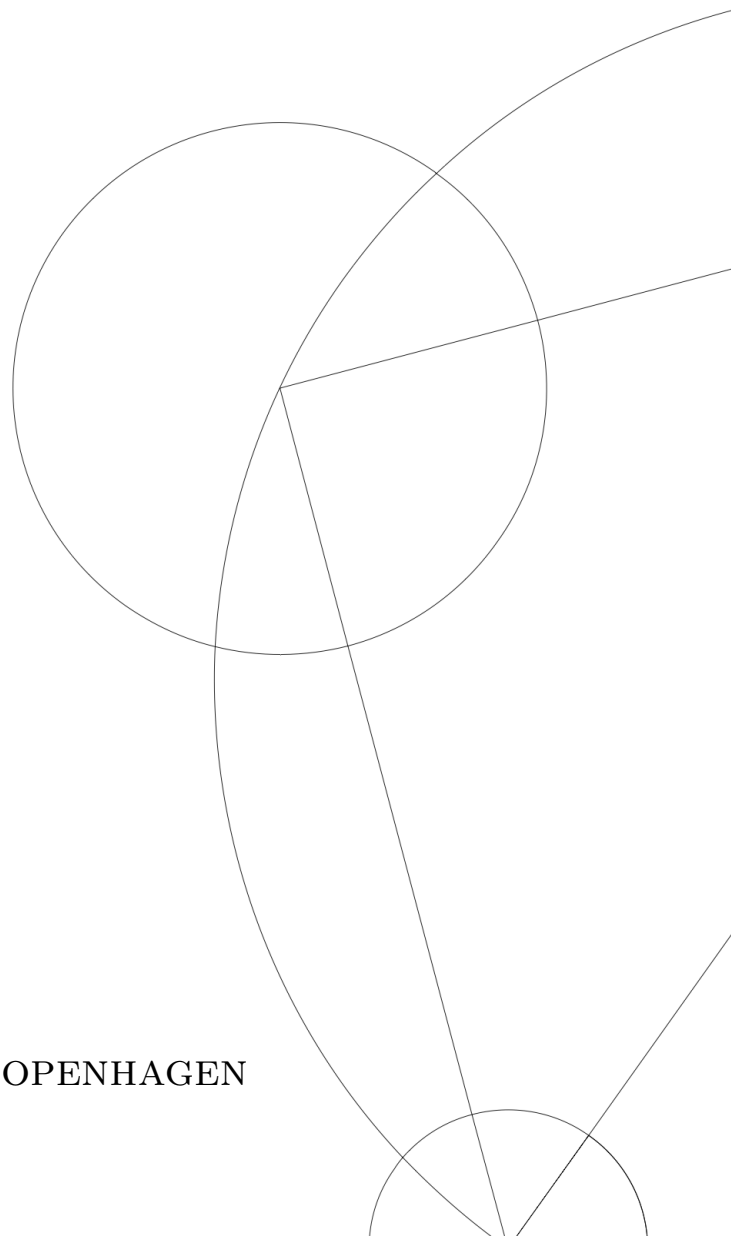

University of Copenhagen

UNIVERSITY OF COPENHAGEN

Faculty:	Faculty of Science
Institute:	Niels Bohr Institute
Author(s):	Cecilie Hermansen
Email:	wtg456@alumni.ku.dk
Title and subtitle:	Vortices in s-Wave Superconductors - A Numerical Study of the Bogoliubov-de Gennes Equations
Supervisor(s):	Brian Møller Andersen
Handed in:	13/06/2018
Defended:	19/06/2018

Name _____

Signature _____

Date _____

Empty your soul and let the universe fill you

Contents

Abstract

When a type II-superconductor is exposed to a magnetic field an Abrikosov vortex lattice forms. This thesis investigates such vortices in an s-wave superconductor modeled by a 2D square lattice with nearest and next-nearest neighbor hopping. The Bogoliubov-de Gennes equations are initially derived and subsequently solved numerically for a system which is subject to a magnetic field. This requires knowledge of second quantization and the microscopic BCS theory of superconductivity. Furthermore, it must be figured out how the hopping constant of the Hamiltonian is modified according to the Peierls substitution in the presence of a magnetic field. The magnetic field affects the translation symmetry of the system as well. Hence the magnetic Bloch theorem must be applied in order to use Born-von Karman boundary conditions. Moreover it is investigated how the complex phase of the superconducting order parameter can be used to determine whether vortices are present in the system. This knowledge is then utilized in the case of a system with impurities on a fraction of the lattice sites. The effect of T_c-enhancement caused by impurities found by Gastiasoro and Andersen [1] is thus investigated and reproduced, as it is confirmed that vortices are sustained above T_c of the homogeneous system.

1. Introduction

Since superconductivity was discovered by Heike Kamerlingh Onnes in 1911 and the first microscopic theory of superconductivity, BCS theory, was presented by Bardeen, Cooper and Schrieffer in 1957, the subject has become a very broad and diverse field of research. In this thesis a type-II superconductor exposed to a magnetic field is studied.

We investigate an s-wave superconductor using the tight-binding model with nearest and next-nearest neighbor hopping in a two-dimensional square lattice. Below the critical temperature this system sustains the formation of vortices, which are encircled by supercurrents. This is shown by solving the Bogoliubov-de Gennes equations numerically in the presence of a nonzero magnetic field. Attaining this requires knowledge of how the magnetic field affects the hopping constants of the Hamiltonian. In order to use Born-von Karman boundary conditions one must also take into account that the translational invariance of the system is broken by the magnetic field. Hence we derive the magnetic Bloch theorem which enables the use of periodic boundary conditions. Furthermore we seek a method of determining whether vortices are present in the system by considering the complex phase of the superconducting order parameter (SCOP). This method is then finally applied to a system with impurities on 15 % of the lattice sites, in order to investigate whether it is possible to reproduce the effect of T_c-enhancement caused by impurities found by Gastiasoro and Andersen [1]. This is the case if it can be confirmed that vortices are present above T_c of the homogeneous system.

2. Theory

2.1. Second quantization

Second quantization is an important formalism in condensed matter physics which will form the basis of almost all derivations in this thesis.[1] The total quantum mechanical wave function for a system of indistinguishable particles must be either symmetric or antisymmetric under particle label exchange, depending on whether one is considering bosons or fermions. In the simple case of a two-particle system with single-particle eigenstates $H\left|\psi_i\right\rangle = \lambda_i \left|\psi_i\right\rangle$ the total symmetric (S)/antisymmetric (A) wave function is given by:

$$\Psi(x_1, x_2)_{\substack{S \\ A}} = \frac{1}{\sqrt{2}}(\psi_1(x_1)\psi_2(x_2) \pm \psi_2(x_1)\psi_1(x_2)). \tag{2.1}$$

Though general expressions for the many-body wave functions in arbitrarily large systems exist (e.g. using Slater determinants for fermions) they quickly become very complicated with increasing particle number. For many-body systems these wave functions are thus practically impossible to use.

Hence we need a new way of constructing the eigenstates. This is done in second quantization with a change of basis to many-particle eigenstates where the number of particles occupying each single-particle eigenstate is sufficient to describe the total state of the system. Defining the vacuum state with no particles $|0\rangle$ we introduce the creation and annihilation operators $c^\dagger_{\lambda_i}$ and c_{λ_i}, which create and annihilate a particle in the eigenstate labeled by quantum numbers λ_i respectively. Thus we can write

[1] The definitions of this section follow the conventions used by [2]

the state with one particle in eigenstate λ_i as:

$$c^\dagger_{\lambda_i} |0\rangle = |0 \quad 0 \quad 0 \ldots \overset{\lambda_i}{1} \ldots 0\rangle. \tag{2.2}$$

So that in second quantization a state is generally given by:

$$|n_{\lambda_1}, n_{\lambda_2}, n_{\lambda_3}, \ldots, n_{\lambda_n}\rangle . \tag{2.3}$$

For bosons the occupation number n_{λ_i} can take any non-negative integer value, whereas for fermions it can only be 0 or 1 due to the Pauli exclusion principle. Hence, applying the same fermion creation (or annihilation) operator twice annihilates the state. The correct symmetrization/antisymmetrization of the wave function is ensured by the (anti-)commutation relations which the creation/annihilation operators satisfy. They are different for fermions and bosons, and since we will be considering electrons in this thesis, only the fermion anticommutation relations are listed here:

$$\{c_{\lambda_i}, c_{\lambda_j}\} = c_{\lambda_i} c_{\lambda_j} + c_{\lambda_j} c_{\lambda_i} = 0 = \{c^\dagger_{\lambda_i}, c^\dagger_{\lambda_j}\} \quad \text{and} \quad \{c_{\lambda_i}, c^\dagger_{\lambda_j}\} = \delta_{\lambda_i \lambda_j}. \tag{2.4}$$

Generally a creation or annihilation operator acts on a state according to:

$$c^\dagger_{\lambda_i} |n_{\lambda_1}\, n_{\lambda_2} \ldots n_{\lambda_i} \ldots\rangle = (-1)^{\sum_i} \sqrt{1 - n_{\lambda_i}}\, |n_{\lambda_1}\, n_{\lambda_2} \ldots . n_{\lambda_i} + 1 \ldots\rangle \tag{2.5}$$

$$c_{\lambda_i} |n_{\lambda_1}\, n_{\lambda_2} \ldots n_{\lambda_i} \ldots\rangle = (-1)^{\sum_i} \sqrt{n_{\lambda_i}}\, |n_{\lambda_1}\, n_{\lambda_2} \ldots . n_{\lambda_i} - 1 \ldots\rangle , \tag{2.6}$$

with $(-1)^{\sum_i} = (-1)^{n_{\lambda_1} + n_{\lambda_2} + \ldots + n_{\lambda_i} - 1}$. Normalization is ensured by the prefactors. In second quantization all single- and many-particle operators can be formulated in terms of the creation and annihilation operators. For example the number operator which counts the number of particles in a given state is:

$$n_{\lambda_i} = \sum_\sigma c^\dagger_{\lambda_i \sigma} c_{\lambda_i \sigma}, \tag{2.7}$$

where the sum is over spin states.

2.2. BCS theory

In BCS theory it is shown that the Fermi surface is unstable to the formation of Cooper pairs due to an attractive electron-electron interaction for electrons near the Fermi surface. The interaction arises from coupling with the phonons of the lattice [3], and it is attractive for electrons with energy $E_F - \hbar\omega_D < E < E_F + \hbar\omega_D$, where ω_D is the Debye frequency. This attraction causes bound states consisting of two electrons just outside the Fermi sea to form. These bound states are the Cooper pairs, and the instability to formation of such pairs causes an energy gap which makes the superconducting state stable below the critical temperature. We will now consider the Hamiltonian of BCS theory, which is given by [4]:

$$H_{BCS} = \sum_{\mathbf{k}\sigma} \varepsilon_{\mathbf{k}} c^\dagger_{\mathbf{k}\sigma} c_{\mathbf{k}\sigma} - \sum_{\mathbf{k}\mathbf{k}'} V_{\mathbf{k}\mathbf{k}'} c^\dagger_{\mathbf{k}\uparrow} c^\dagger_{-\mathbf{k}\downarrow} c_{-\mathbf{k}'\downarrow} c_{\mathbf{k}'\uparrow}, \tag{2.8}$$

where $V_{\mathbf{k}\mathbf{k}'} = -V$ for $|\varepsilon_{\mathbf{k}}| < \hbar\omega_D$ and $\varepsilon_{\mathbf{k}} = \frac{\hbar^2 k^2}{2m} - \mu$. The first term is just the single-particle energy, and the second term is an interaction term which describes scattering between Cooper pairs of momentum $(\mathbf{k}, -\mathbf{k})$ and $(\mathbf{k}', -\mathbf{k}')$. This interaction term makes it impossible to diagonalize the Hamiltonian. Hence

we perform a mean-field decoupling of the interaction term. By introducing

$$\Delta = V \sum_{\mathbf{k}'} \langle c_{-\mathbf{k}'\downarrow} c_{\mathbf{k}'\uparrow} \rangle, \tag{2.9}$$

and absorbing a term $\langle c^\dagger_{\mathbf{k}\uparrow} c^\dagger_{-\mathbf{k}\downarrow} \rangle \langle c_{-\mathbf{k}\downarrow} c_{\mathbf{k}\uparrow} \rangle$ into the chemical potential the mean-field Hamiltonian is obtained:

$$H^{MF}_{BCS} = \sum_{\mathbf{k}\sigma} \varepsilon_{\mathbf{k}} c^\dagger_{\mathbf{k}\sigma} c_{\mathbf{k}\sigma} - \sum_{\mathbf{k}} \Delta c^\dagger_{\mathbf{k}\uparrow} c^\dagger_{-\mathbf{k}\downarrow} - \sum_{\mathbf{k}} \Delta^* c_{-\mathbf{k}\downarrow} c_{\mathbf{k}\uparrow}. \tag{2.10}$$

This can be written in matrix form (using that $\varepsilon_{-\mathbf{k}} = \varepsilon_{\mathbf{k}}$ if the crystal is invariant under the substitution $\mathbf{r} \to -\mathbf{r}$ which is usually the case):

$$H^{MF}_{BCS} = \sum_{\mathbf{k}} \begin{pmatrix} c^\dagger_{\mathbf{k}\uparrow} & c_{-\mathbf{k}\downarrow} \end{pmatrix} \begin{pmatrix} \varepsilon_{\mathbf{k}} & -\Delta \\ -\Delta^* & -\varepsilon_{\mathbf{k}} \end{pmatrix} \begin{pmatrix} c_{\mathbf{k}\uparrow} \\ c^\dagger_{-\mathbf{k}\downarrow} \end{pmatrix}. \tag{2.11}$$

Our aim is now to diagonalize the Hamiltonian, and this can be done by introducing the unitary transformation U:

$$U = \begin{pmatrix} u_{\mathbf{k}} & v^*_{\mathbf{k}} \\ -v_{\mathbf{k}} & u^*_{\mathbf{k}} \end{pmatrix}, \tag{2.12}$$

which we then demand diagonalizes the Hamiltonian so that:

$$U^\dagger \begin{pmatrix} \varepsilon_{\mathbf{k}} & -\Delta \\ -\Delta^* & -\varepsilon_{\mathbf{k}} \end{pmatrix} U = \begin{pmatrix} E_{\mathbf{k}} & 0 \\ 0 & -E_{\mathbf{k}} \end{pmatrix}. \tag{2.13}$$

This gives a set of equations which can be solved by parameterizing according to $u_{\mathbf{k}} = \cos(t)$ and $v_{\mathbf{k}} = \sin(t)$ and using that U is unitary, so that $|u_{\mathbf{k}}|^2 + |v_{\mathbf{k}}|^2 = 1$. Furthermore we assume that $u_{\mathbf{k}}$ and $v_{\mathbf{k}}$ can be taken to be real, which is always true in the spatially uniform case where $\mathbf{k}$ is a good quantum number. We then get that:

$$E_{\mathbf{k}} = \sqrt{\varepsilon^2_{\mathbf{k}} + |\Delta|^2}, \tag{2.14}$$

$$|u_{\mathbf{k}}| = \sqrt{\frac{1}{2}\left(1 + \frac{\varepsilon_{\mathbf{k}}}{E_{\mathbf{k}}}\right)} \quad \text{and} \quad |v_{\mathbf{k}}| = \sqrt{\frac{1}{2}\left(1 - \frac{\varepsilon_{\mathbf{k}}}{E_{\mathbf{k}}}\right)}. \tag{2.15}$$

The diagonalization is equivalent to performing a transformation of the original operators to a set of new fermionic creation and annihilation operators:

$$\begin{pmatrix} \gamma_{\mathbf{k}\uparrow} \\ \gamma^\dagger_{-\mathbf{k}\downarrow} \end{pmatrix} = U^\dagger \begin{pmatrix} c_{\mathbf{k}\uparrow} \\ c^\dagger_{-\mathbf{k}\downarrow} \end{pmatrix}, \tag{2.16}$$

and the Hamiltonian is diagonal in these new operators:

$$H^{MF}_{BCS} = \sum_{\mathbf{k}} E_{\mathbf{k}} \gamma^\dagger_{\mathbf{k}\sigma} \gamma_{\mathbf{k}\sigma}. \tag{2.17}$$

The interpretation of this term is that it determines the number of excitations above the superconducting ground state with energy $E_{\mathbf{k}} > 0$. The $\gamma_{\mathbf{k}\sigma}-$operators represent the Bogoliubon quasiparticles, which can be interpreted as a superposition of an electron and a hole. If the charge of the excitation is measured, $|v_{\mathbf{k}}|^2$ is the probability of measuring an electron and $|u_{\mathbf{k}}|^2$ is the probability of measuring a hole [3]. Since

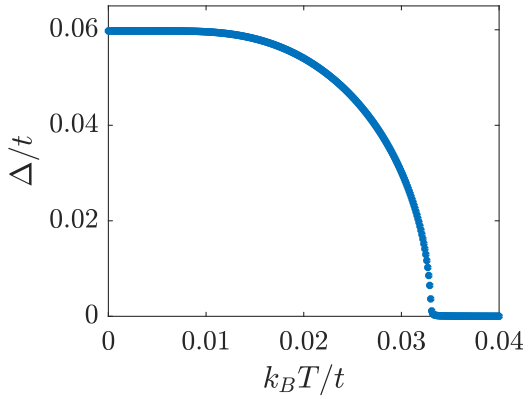

Figure 2.1.: The superconducting order parameter as a function of temperature in a 2D square lattice. At the critical temperature the order parameter drops to zero, and a phase transition to the normal state occurs.

the γ-operators represent fermions their thermal averages are:

$$\langle \gamma^\dagger_{\mathbf{k}\sigma}\gamma_{\mathbf{k}'\sigma'}\rangle = f(E_\mathbf{k})\delta_{\mathbf{k}\mathbf{k}'}\delta_{\sigma\sigma'} \quad \text{and} \quad \langle \gamma^\dagger_{\mathbf{k}\sigma}\gamma^\dagger_{\mathbf{k}'\sigma'}\rangle = 0. \tag{2.18}$$

We can now write Δ, which is the gap parameter of the superconductor, in terms of the new operators:

$$\Delta = V\sum_\mathbf{k} u_\mathbf{k} v^*_\mathbf{k}(1-2f(E_\mathbf{k})) = V\sum_\mathbf{k}\frac{\Delta}{2E_\mathbf{k}}\tanh\left(\frac{E_\mathbf{k}}{2k_BT}\right), \tag{2.19}$$

where in the last step it was used that the Fermi distribution is given by $f(E_\mathbf{k}) = \frac{1}{\exp(E_\mathbf{k}/k_BT)+1}$ and the expressions for $u_\mathbf{k}$ and $v_\mathbf{k}$ in eq. 2.15 were substituted. Δ is the superconducting order parameter which is only nonzero below the critical temperature T_c (the energy gap vanishes at T_c), and eq. 2.19 is the self-consistency equation which must be solved in order to determine the value of the superconducting order parameter at different temperatures. In the homogeneous case this can be done analytically at $T = 0$, and by exploiting that Δ vanishes at the critical temperature, an expression for k_BT_c can also be found in the weak-coupling limit. See Appendix A for more details on this.
One can then derive the so-called BCS ratio: $\frac{2\Delta(0)}{kT_c} = 3.52$, which has been experimentally verified for conventional low-T_c superconductors and is thus a great success of BCS theory. For homogeneous systems, the superconducting order parameter as a function of temperature can easily be determined by numerically solving the self-consistency equation in eq. 2.19. We have done this for a 2D square lattice in the tight-binding model with 1000 sites in both the x- and y-direction and lattice constant $a = 1$. The electron energies $\varepsilon_\mathbf{k}$ are given by the dispersion relation $\varepsilon_\mathbf{k} = -2t(\cos(k_xa) + \cos(k_ya))$, where k_x and k_y are in the first Brillouin zone [5]. See fig. 2.1 for a plot of Δ as a function of temperature. The BCS ratio found from the calculations is $\frac{2\Delta(0)}{kT_c} = 3.59$, where the deviation from the theoretical value is likely due to the finite size of the system.

2.3. The Hamiltonian

The calculations presented above are more complicated in the case where the system is not spatially uniform, which is the case to be considered next. The Hamiltonian describing s-wave superconductivity[2] in a two-dimensional square lattice using the tight-binding model is given by:

[2]Cooper pairs with spin singlet pairing and no relative angular momentum of the electrons.

$$H = -\sum_{ij\sigma} t_{ij} c^\dagger_{i\sigma} c_{j\sigma} + \sum_{i\sigma} (V^{\text{imp}}_{i\sigma} - \mu) c^\dagger_{i\sigma} c_{i\sigma} - V \sum_i c^\dagger_{i\uparrow} c_{i\uparrow} c^\dagger_{i\downarrow} c_{i\downarrow} = H_1 + H_2 + H_3, \tag{2.20}$$

where $c^\dagger_{i\sigma}$ and $c_{i\sigma}$ create and annihilate a particle at site i respectively. The first term H_1 is the kinetic energy. t_{ij} is the hopping integral which is a measure of how likely it is for the electron to tunnel to another atom in the lattice. Hopping to nearest ($t_{ij} = t$) and next-nearest neighbors ($t_{ij} = t'$) is included. t and t' are real and we will let $t > 0$ and $t' < 0$. However, this simple form of the hopping integral only applies to the case where no B-field is applied. If there *is* a B-field, a complex phase needs to be introduced. This situation will be treated in detail below. The second term is the on-site energy where $V^{\text{imp}}_{i\sigma}$ is the impurity strength and μ is the chemical potential. The third term is the BCS-term which describes the scattering between Cooper pairs on the same site i. The s-wave superconductivity arises from this term. Again $V < 0$ so that the electron-electron interaction is attractive. As is evident from eq. 2.20, the Hamiltonian is not quadratic in the creation and annihilation operators, and thus it is not possible to solve the corresponding Schrödinger equation analytically. Hence we perform a mean-field decoupling of the last term [2]

$$H_3^{MF} = -V \sum_i \left[\Delta^*_i c_{i\downarrow} c_{i\uparrow} + \Delta_i c^\dagger_{i\uparrow} c^\dagger_{i\downarrow} \right], \tag{2.21}$$

where

$$\Delta_i = V \langle c_{i\downarrow} c_{i\uparrow} \rangle \text{ and } \Delta^*_i = V \langle c^\dagger_{i\uparrow} c^\dagger_{i\downarrow} \rangle. \tag{2.22}$$

With this mean-field decoupling of the BCS Hamiltonian, H is now quadratic in the creation and annihilation operators and can be diagonalized. As was previously remarked, this can not be done by following the method outlined in section 2.2 when the system is inhomogeneous (due to e.g. a magnetic field or impurities). For this reason the Bogoliubov-de Gennes equations are introduced. As will be shown in the following section, diagonalizing the Hamiltonian corresponds to solving the Bogoliubov-de Gennes equations.

2.4. Bogoliubov-de Gennes equations

The purpose of solving the Bogoliubov-de Gennes equations is to find the unitary transformation which diagonalizes the Hamiltonian. For a homogeneous system this is rather uncomplicated as we know that in that situation $\mathbf{k}$ is a good quantum number, and the transformation we need is the Bogoliubov transformation used in the previous section. However, in the case where a magnetic field or impurities are present, the system is no longer homogeneous and $\mathbf{k}$ is not a good quantum number. Thus we need to introduce a more general transformation:

$$c_{i\sigma} = \sum_n \left[u_{n,i\sigma} \gamma_{n\sigma} + v^*_{n,i\sigma} \gamma^\dagger_{n\bar{\sigma}} \right], \tag{2.23}$$

where n is the set of good quantum numbers which are not known. We now require that the Hamiltonian is diagonal in the γ-operators. That is:

$$H^{MF} = E_0 + \sum_{n\sigma} E_{n\sigma} \gamma^\dagger_{n\sigma} \gamma_{n\sigma}. \tag{2.24}$$

This is only obtained for certain values of u_n and v_n in the transformation above. By solving the Bogoliubov-de Gennes equations these values are determined. The equations are derived by calculating

the commutators of the Hamiltonians in eq. 2.20 and 2.24 with the creation and annihilation operators. The γ-operators are fermion operators so the usual anticommutation relations in eq. 2.4 apply. Using this we easily obtain:

$$\begin{aligned}\left[H^{MF}, \gamma_{n\sigma}\right] &= -E_{n\sigma}\gamma_{n\sigma}, \\ \left[H^{MF}, \gamma^{\dagger}_{n\sigma}\right] &= E_{n\sigma}\gamma^{\dagger}_{n\sigma}.\end{aligned} \tag{2.25}$$

The commutators of eq. 2.20 with the creation and annihilation operators are derived in a completely similar manner, using the fermion anticommutation relations and the following identity for fermions: $[AB, C] = A\{B, C\} - \{A, C\}B$. The calculations are somewhat lengthy and we refer to appendix B for the details. The final result is that the commutators are given by:

$$\begin{aligned}[H, c_{i\uparrow}] &= \sum_j t_{ij}c_{j\uparrow} - (V^{\text{imp}}_{i\uparrow} - \mu)c_{i\uparrow} + \Delta_i c^{\dagger}_{i\downarrow}, \\ [H, c_{i\downarrow}] &= \sum_j t_{ij}c_{j\downarrow} - (V^{\text{imp}}_{i\downarrow} - \mu)c_{i\downarrow} - \Delta_i c^{\dagger}_{i\uparrow}.\end{aligned} \tag{2.26}$$

By substituting the transformation in eq. 2.23 into eq. 2.26 and demanding the commutators in eq. 2.25 and 2.26 to be equal we obtain the four Bogoliubov-de Gennes equations:

$$\begin{aligned}E_{n\uparrow}u_{n,i\uparrow} &= -\sum_j t_{ij}u_{n,j\uparrow} + (V^{\text{imp}}_{i\uparrow} - \mu)u_{n,i\uparrow} - \Delta_i v_{n,i\downarrow}, \\ E_{n\downarrow}v^*_{n,i\uparrow} &= \sum_j t_{ij}v^*_{n,j\uparrow} - (V^{\text{imp}}_{i\uparrow} - \mu)v^*_{n,i\uparrow} + \Delta_i u^*_{n,i\downarrow}, \\ E_{n\downarrow}u_{n,i\uparrow} &= -\sum_j t_{ij}u_{n,j\downarrow} + (V^{\text{imp}}_{i\downarrow} - \mu)u_{n,i\downarrow} + \Delta_i v_{n,i\uparrow}, \\ E_{n\uparrow}v^*_{n,i\downarrow} &= \sum_j t_{ij}v^*_{n,j\downarrow} - (V^{\text{imp}}_{i\downarrow} - \mu)v^*_{n,i\downarrow} - \Delta_i u^*_{n,i\uparrow}.\end{aligned} \tag{2.27}$$

Defining the operator

$$\hat{h}_\sigma u_{i\sigma} = -\sum_j t_{ij}u_{j\sigma} + (V^{\text{imp}}_{i\sigma} - \mu)u_{i\sigma}, \tag{2.28}$$

the four eqs. 2.27 can be written in matrix form:

$$\begin{pmatrix} \hat{h}_\uparrow & -\Delta_i \\ -\Delta^*_i & -\hat{h}^*_\downarrow \end{pmatrix} \begin{pmatrix} u_{n\uparrow} \\ v_{n\downarrow} \end{pmatrix} = E_{n\uparrow} \begin{pmatrix} u_{n\uparrow} \\ v_{n\downarrow} \end{pmatrix} \tag{2.29}$$

and

$$\begin{pmatrix} \hat{h}_\downarrow & \Delta_i \\ \Delta^*_i & -\hat{h}^*_\uparrow \end{pmatrix} \begin{pmatrix} u_{n\downarrow} \\ v_{n\uparrow} \end{pmatrix} = E_{n\downarrow} \begin{pmatrix} u_{n\downarrow} \\ v_{n\uparrow} \end{pmatrix}. \tag{2.30}$$

As shown in appendix C it is only necessary to solve one of the eqs. 2.29 or 2.30, because if $\left(\begin{smallmatrix} u_{n\uparrow} \\ v_{n\downarrow} \end{smallmatrix}\right)$ is an eigenvector of the matrix in eq. 2.29 with a negative eigenvalue $-E_{n\uparrow}$, $\left(\begin{smallmatrix} v^*_{n\uparrow} \\ u^*_{n\downarrow} \end{smallmatrix}\right)$ is an eigenvector of the matrix in eq. 2.30 with a positive eigenvalue $E_{n\downarrow}$. So in the numerical calculations, we only need to solve eq. 2.30. The order parameter can also be determined in terms of $u_{n,i\sigma}$ and $v_{n,i\sigma}$ by invoking the transformation in eq. 2.22, and the expectation values in eq. 2.18:

$$\begin{aligned}\Delta_i = V\langle c_{i\downarrow}c_{i\uparrow}\rangle &= V\sum_n \Big\langle \Big(u_{n,i\downarrow}\gamma_{n\downarrow} + v^*_{n,i\downarrow}\gamma^\dagger_{n\uparrow})(u_{n,i\uparrow}\gamma_{n\uparrow} + v^*_{n,i\uparrow}\gamma^\dagger_{n\downarrow}\Big)\Big\rangle \\ &= V\sum_n \Big[u_{n,i\downarrow}v^*_{n,i\uparrow}f(-E_{n\downarrow}) + v^*_{n,i\downarrow}u_{n,i\uparrow}f(E_{n\uparrow})\Big].\end{aligned} \tag{2.31}$$

Using the correspondence between positive and negative eigenvalues and suppressing the spin indices, (as the eigenstates of the system are spin degenerate) we get:

$$\Delta_i = V\sum_{n,E_n<0} u_{n,i}v^*_{n,i}f(E_n) + V\sum_{n,E_n>0} u_{n,i}v^*_{n,i}f(E_n) = V\sum_l u_{l,i}v^*_{l,i}f(E_l), \tag{2.32}$$

Where the last sum is over both positive and negative eigenvalues. Another self-consistent quantity is the density of electrons at a site i of the lattice, which is derived in appendix D:

$$\langle\hat{n}_i\rangle = \sum_l \Big[|u_{l,i}|^2 f(E_l) + |v_{l,i}|^2(1-f(E_l))\Big]. \tag{2.33}$$

The chemical potential can be adjusted to give the desired electron density.

3. Magnetic field

3.1. Peierls phases

When a magnetic field is applied to the system, the momentum operator $\mathbf{p}$ is shifted according to $\mathbf{p} \to \mathbf{p} + e\mathbf{A}(\mathbf{r})$ [6], where $\mathbf{A}$ is the vector potential and $\mathbf{B} = \nabla \times \mathbf{A}$. Hence the Hamiltonian is no longer invariant under discrete translations by one lattice vector, because even if the magnetic field is uniform, the vector potential is not invariant under such translations. The consequence of this is that the hopping constant t_{ij} gains a complex phase known as the Peierls phase, which will be derived in this section following the procedure from [7].

Only the tight-binding part of the Hamiltonian is considered in what follows. In the presence of a static magnetic field, the second quantized Hamiltonian is given by:

$$H = \int d\mathbf{r}\psi^\dagger_\alpha(\mathbf{r})h_\sigma(\mathbf{r})\psi_\alpha(\mathbf{r}), \tag{3.1}$$

where

$$\psi_\alpha(\mathbf{r}) = \sum_i a(\mathbf{r}-\mathbf{R}_i)c_{i\alpha} \quad \text{and} \quad \psi_\alpha(\mathbf{r})^\dagger = \sum_i a(\mathbf{r}-\mathbf{R}_i)c^\dagger_{i\alpha} \tag{3.2}$$

are the field operators. $a(\mathbf{r}-\mathbf{R_i})$ are the atomic orbitals on site i of the lattice. They are localized at $\mathbf{R_i}$ and fall off rapidly as the distance $\mathbf{r}-\mathbf{R_i}$ increases. The single-particle Hamiltonian is

$$h_\alpha = \frac{1}{2m}\left(\mathbf{p} + e\mathbf{A}(\mathbf{r})\right)^2 + V(\mathbf{r}) - E_F. \tag{3.3}$$

$V(\mathbf{r})$ is the Coulomb potential produced by the atoms in the lattice and $\mathbf{p} = \frac{\hbar}{i}\nabla_\mathbf{r}$ is the momentum operator. Expanding the parenthesis in eq. 3.3 we get: $(\mathbf{p}+e\mathbf{A}(\mathbf{r}))^2 = \mathbf{p}^2 + e^2\mathbf{A}^2 + \mathbf{p}\cdot\mathbf{A} + \mathbf{A}\cdot\mathbf{p}$ Hence it is seen that the nonzero vector potential causes cross terms $\mathbf{p}\cdot\mathbf{A}$ and $\mathbf{A}\cdot\mathbf{p}$ to arise, which complicates all calculations greatly. For this reason, our goal is now to find a gauge transformation which allows us to write the Hamiltonian on the usual tight-binding form. That is, a gauge transformation which cancels the cross terms. In order for the Schrödinger equation to be gauge invariant a gauge transformation of

the vector potential

$$\mathbf{A} \to \mathbf{A} + \nabla\Lambda(\mathbf{r}) \tag{3.4}$$

requires a similar transformation

$$\psi_\nu(\mathbf{r}) \to \psi_\nu(\mathbf{r}) e^{-i\frac{e}{\hbar}\Lambda(\mathbf{r})} \tag{3.5}$$

of the wave function [8]. The field operators (now characterized by the spin quantum number σ) transform accordingly:

$$\psi_\sigma(\mathbf{r}) = \sum_i a(\mathbf{r} - \mathbf{R_i}) e^{-i\frac{e}{\hbar}\Lambda_i} c_{i\sigma} \tag{3.6}$$

The scalar field Λ_i is the generator of the gauge transformation. Claiming that the generator

$$\Lambda_i = \int_{\mathbf{R}_i}^{\mathbf{r}} \mathbf{A}(\mathbf{r}')d\mathbf{r}' = \int_0^1 (\mathbf{r} - \mathbf{R}_i) \cdot \mathbf{A}(\mathbf{R_i} + \lambda(\mathbf{r} - \mathbf{R_i}))d\lambda \tag{3.7}$$

satisfies our requirements will eventually lead to an expression for the Peierls phase. In the second equality the integral was transformed to a line integral along the straight line joining $\mathbf{r}$ and $\mathbf{R_i}$ using the parametrization $\mathbf{r}' = \lambda(\mathbf{r} - \mathbf{R}_i) + \mathbf{R}_i$. After some lengthy calculations which can be seen in Appendix E, we find that the Hamiltonian in eq. 3.1 can be written as:

$$\begin{aligned} H &= \int d\mathbf{r} \sum_{i\sigma} a^*(\mathbf{r} - \mathbf{R}_i) e^{i\frac{e}{\hbar}\Lambda_i} c^\dagger_{i\sigma} \left[\frac{1}{2m} \left(\frac{\hbar}{i}\nabla_{\mathbf{r}} + e\mathbf{A}(\mathbf{r}) \right) + V(\mathbf{r}) - E_F \right] \sum_{j\sigma} a(\mathbf{r} - \mathbf{R}_j) e^{-i\frac{e}{\hbar}\Lambda_j} c_{j\sigma} \\ &= \sum_{ij\sigma} \tilde{h}_{ij} c^\dagger_{i\sigma} c_{j\sigma}, \end{aligned} \tag{3.8}$$

where

$$\begin{aligned} \tilde{h}_{ij} = \int d\mathbf{r} a^*(\mathbf{r} - \mathbf{R_i}) e^{i\frac{e}{\hbar}(\Lambda_i - \Lambda_j)} \Bigg[\frac{1}{2m} \big(\mathbf{p} - e \int_0^1 d\lambda\, \lambda(\mathbf{r} - \mathbf{R_j}) \times \mathbf{B}(\mathbf{R_j} + \lambda(\mathbf{r} - \mathbf{R_j})) \big)^2 \\ + V(\mathbf{r}) - E_F \Bigg] a(\mathbf{r} - \mathbf{R_j}) \end{aligned} \tag{3.9}$$

is the single-particle Hamiltonian in the presence of a magnetic field. Hence we are able to express the Hamiltonian on the usual tight-binding form even though the single-particle Hamiltonian now contains some complicated terms arising from the gauge transformation. But if the B-field is slowly varying (in our case it is constant), the fact that the atomic orbitals are localized allows for the approximation $\mathbf{r} \simeq \mathbf{R_j}$ in the λ-integral in eq. 3.9. Hence we get no contribution from this term, and the single-particle Hamiltonian becomes

$$\tilde{h}_{ij} = -t_{ij} e^{i\phi_{ij}} + (\varepsilon_i - E_F)\delta_{ij}, \tag{3.10}$$

where the last term is the on-site energy and

$$t_{ij} = -\int d\mathbf{r} a^*(\mathbf{r} - \mathbf{R_i}) \left(\frac{\mathbf{p}^2}{2m} + V(\mathbf{r}) \right) a(\mathbf{r} - \mathbf{R_j}), \tag{3.11}$$

is the hopping integral in the absence of a magnetic field.

$$\phi_{ij} = -\frac{e}{\hbar} \int_{\mathbf{R_j}}^{\mathbf{R_i}} \mathbf{A}(\mathbf{r}) \cdot d\mathbf{r} = -\frac{2\pi}{\Phi_0} \int_{\mathbf{R_j}}^{\mathbf{R_i}} \mathbf{A}(\mathbf{r}) \cdot d\mathbf{r} \tag{3.12}$$

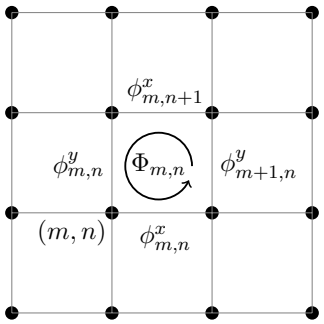

Figure 3.1.: An electron which tunnels along the borders of a unit cell picks up a phase which is related to the flux through the unit cell Φ_{mn}. The unit cell is labeled by the indices of the lower left corner (m, n)

is the Peierls phase which we set out to obtain and $\Phi_0 = \frac{h}{e}$ is the flux quantum. Through a gauge transformation it has thus been shown that in the presence of a magnetic field it is possible to express the tight-binding Hamiltonian on a form which is similar to the case of no magnetic field. However, the hopping integral has to be modified according to the Peierls substitution:

$$t_{ij} \to t_{ij} e^{-i\frac{2\pi}{\Phi_0}\int_{\mathbf{R_j}}^{\mathbf{R_i}} \mathbf{A}(\mathbf{r})\cdot d\mathbf{r}}. \tag{3.13}$$

This result can be understood intuitively in reference to the Aharonov-Bohm effect which concerns the fact that a particle traveling in a region of nonzero vector potential gains a complex phase depending on the path it takes.

3.2. Magnetic Bloch theorem

In a lattice which is invariant under translations by a lattice vector Bloch's theorem applies. This means that translating the wave function by a lattice vector $\mathbf{R} = n_1\mathbf{a_1} + n_2\mathbf{a_2}$ is equivalent to multiplying it by a complex phase [9], that is $\psi(\mathbf{r} + \mathbf{R}) = e^{i\mathbf{k}\cdot\mathbf{R}}\psi(\mathbf{r})$. This is due to the fact that the translation operators commute with each other and with the Hamiltonian. The Hamiltonian and the translation operators thus have simultaneous eigenstates which are periodic in the unit cells of the lattice and are labeled by the momentum quantum number $\mathbf{k}$. However, when a magnetic field is applied the translational invariance is broken, because even if the B-field is uniform the vector potential and hence also the Peierls phases are position dependent. In this section we will derive a magnetic Bloch theorem which takes this effect into account. In the following we will denote a site by its indices in the x- and y-direction (m, n). The x- and y-components of the Peierls phase for hopping by one primitive lattice vector from site (m, n) are $\phi^i_{m,n}$, $i = \{x, y\}$. We will also need to know the flux per plaquette (unit cell of the original lattice). An electron which tunnels along the borders of a unit cell picks up a phase which is related to the flux through the unit cell, $\Phi_{m,n}$ (see fig. 3.1 for an illustration of this):

$$\begin{aligned} &\phi^x_{m,n} + \phi^y_{m+1,n} - \phi^x_{m,n+1} - \phi^y_{m,n} \\ &= \frac{2\pi}{\Phi_0}\oint_{\text{unit cell}} \mathbf{A}(\mathbf{r})\cdot d\mathbf{r} \\ &= \frac{2\pi}{\Phi_0}\int_{\text{unit cell}} \mathbf{B}\cdot d\mathbf{S} = \frac{2\pi}{\Phi_0}\Phi_{m,n}. \end{aligned} \tag{3.14}$$

(m, n) are the indices of the site in the lower left corner of the unit cell. From now on we will use $\Phi_{m,n}$ to denote the flux per plaquette in units of the flux quantum $\Phi_0 = \frac{h}{e}$. Only the tight-binding part of the

Hamiltonian is affected by the magnetic field. Hence the Hamiltonian to be considered is:

$$H = -t\sum_{m,n}\left(e^{i\phi^x_{m,n}}c^\dagger_{m+1,n}c_{m,n} + e^{i\phi^y_{m,n}}c^\dagger_{m,n+1}c_{m,n} + H.c.\right) \quad = \hat{T}_x + \hat{T}_y + H.c., \tag{3.15}$$

where

$$\hat{T}_x = \sum_{m,n} e^{i\phi^x_{m,n}}c^\dagger_{m+1,n}c_{m,n} \quad \text{and} \quad \hat{T}_y = \sum_{m,n} e^{i\phi^y_{m,n}}c^\dagger_{m,n+1}c_{m,n} \tag{3.16}$$

are the translation operators which translate by a primitive lattice vector in the x- and y-direction respectively. Only nearest-neighbor hopping is included, but the results generalize to next-nearest neighbor hopping. In order to formulate the magnetic Bloch theorem it is necessary to find new translation operators which commute with each other and with the Hamiltonian given above. Following the procedure in [10], we construct the general magnetic translation operators (MTO's):

$$T^M_x = \sum_{m,n} c^\dagger_{m+1,n}c_{m,n}e^{i\theta^x_{m,n}} \quad \text{and} \quad T^M_y = \sum_{m,n} c^\dagger_{m,n+1}c_{m,n}e^{i\theta^y_{m,n}}. \tag{3.17}$$

The effect of these operators is a combination of a gauge transformation and a translation. The aim is now to determine the phases θ^i_{mn} so that the relevant commutators vanish:

$$\left[T^M_x, T^M_y\right] = 0 \quad \text{and} \quad \left[T^M_x, H\right] = \left[T^M_y, H\right] = 0. \tag{3.18}$$

As is shown in Appendix F, this condition is satisfied if the phases

$$\theta^x_{m,n} = \phi^x_{m,n} + 2\pi\Phi_{m,n}n, \tag{3.19}$$

$$\theta^y_{m,n} = \phi^y_{m,n} - 2\pi\Phi_{m,n}m, \tag{3.20}$$

are used. It is now ensured that the magnetic translation operators commute with the Hamiltonian, but not necessarily with each other. Hence we need to make sure that this is also the case. We calculate $T^M_xT^M_y$ and $T^M_yT^M_x$ by applying these operators to a single particle state on site (m,n) given by $\psi_{m,n} = c^\dagger_{m,n}\left|0\right\rangle$:

$$T^M_xT^M_y\psi_{m,n} = T^M_xe^{i\theta^y_{m,n}}\psi_{m,n+1} = e^{i\theta^x_{m,n+1}}e^{i\theta^y_{m,n}}\psi_{m+1,n+1}, \tag{3.21}$$

$$T^M_yT^M_x\psi_{m,n} = e^{i\theta^x_{m,n}}e^{i\theta^y_{m+1,n}}\psi_{m+1,n+1}. \tag{3.22}$$

Let us now consider the specific case of a homogeneous magnetic field, where the flux per plaquette is simply denoted $\Phi_{m,n} = \Phi$. By plugging eqs. 3.19 and 3.20 into eqs. 3.21 and 3.22 we get

$$\begin{aligned} T^M_xT^M_y\psi_{m,n} &= e^{i(\phi^x_{m,n+1}+2\pi\Phi_{m,n+1}(n+1)+\phi^y_{m,n}-2\pi\Phi_{m,n}m)}\psi_{m+1,n+1} \\ &= e^{i(\phi^x_{m,n+1}+2\pi\Phi(n+1)+\phi^y_{m,n}-2\pi\Phi m)}\psi_{m+1,n+1} \end{aligned} \tag{3.23}$$

and

$$\begin{aligned} T^M_yT^M_x\psi_{m,n} &= e^{i(\phi^x_{m,n}+2\pi\Phi_{m,n}n+\phi^y_{m+1,n}-2\pi\Phi_{m+1,n}(m+1))}\psi_{m+1,n+1} \\ &= e^{i(\phi^x_{m,n}+2\pi\Phi n+\phi^y_{m+1,n}-2\pi\Phi(m+1))}\psi_{m+1,n+1}. \end{aligned} \tag{3.24}$$

Combining eqs. 3.23 and 3.24 and using that the flux per plaquette is given by eq. 3.14 we obtain:

$$\begin{aligned}\frac{T_x^M T_y^M \psi_{m,n}}{T_y^M T_x^M \psi_{m,n}} &= e^{i(\phi^x_{m,n+1}+\phi^y_{m,n}-\phi^x_{m,n}-\phi^y_{m+1,n}+4\pi\Phi)} \\ &\implies T_x^M T_y^M e^{-i2\pi\Phi} = T_y^M T_x^M .\end{aligned} \tag{3.25}$$

Hence the magnetic translation operators commute if the flux per plaquette is an integer number of flux quanta. However, this is gauge-equivalent to the trivial case of zero flux per plaquette, which is not the case we are interested in. But even if this condition is not satisfied we can get the MTO's to commute by constructing a larger unit cell, that is, we can apply the magnetic translation operators multiple times. This new unit cell is denoted the magnetic unit cell (MUC) of the system, and there are in general several possible choices. We use a general MUC of dimension $N_x \times N_y$. A translation by a primitive lattice vector of the new lattice of MUC's corresponds to applying T_x^M N_x times and T_y^M N_y times. We can then generalize eq. 3.25 according to:

$$\left(T_x^M\right)^{N_x}\left(T_y^M\right)^{N_y} e^{-i2\pi N_x N_y \Phi} = \left(T_y^M\right)^{N_y}\left(T_x^M\right)^{N_x} . \tag{3.26}$$

The translation operators generally only commute if the flux per plaquette is rational, that is $\Phi = \frac{p}{q}$ [10] with p and q relatively prime, so that:

$$N_x N_y \Phi = N_x N_y \frac{p}{q} \stackrel{!}{=} \nu, \quad \nu \in \mathbb{Z}. \tag{3.27}$$

The smallest possible MUC which satisfies this is one of area $N_x N_y = q$.
As $N_x N_y \Phi$ is the flux through each magnetic unit cell in units of the flux quantum, this condition is equivalent to requiring that the flux through each MUC is an integer number of flux quanta. For the specific case of a uniform magnetic field in the Landau gauge $\mathbf{A} = (0, Bx, 0) = (0, 2\pi\Phi m, 0)$ the phases in eqs. 3.19 and 3.20 become

$$\theta^x_{mn} = 2\pi n\phi, \tag{3.28}$$

$$\theta^y_{mn} = 2\pi m\Phi - 2\pi m\Phi = 0. \tag{3.29}$$

Only the area and not the dimensions of the MUC are fixed by the condition in eq. 3.27, so one is free to choose a unit cell which contains q sites in the x-direction and one site in the y-direction. The commuting operators are then

$$(T_x^M)^q = \sum_{m,n} e^{i2\pi q n\Phi} c^\dagger_{m+q,n} c_{m,n}, \tag{3.30}$$

$$T_y^M = \sum_{m,n} c^\dagger_{m,n+1} c_{m,n}. \tag{3.31}$$

Defining two different lattice vectors of the lattice of MUC's: $\mathbf{R}_m = m_x q\mathbf{a}_x + m_y\mathbf{a}_y$ and $\mathbf{R}_n = n_x q\mathbf{a}_x + n_y\mathbf{a}_y$, it can also be shown that the MTO's satisfy the relation [11]

$$T^M_{\mathbf{R}_m} T^M_{\mathbf{R}_n} = T^M_{\mathbf{R}_m+\mathbf{R}_n},$$

which is necessary in order to be able to formulate the magnetic Bloch theorem.
Due to the translation operators and the Hamiltonian being commuting operators, they have simultaneous eigenstates, and these eigenstates are the magnetic Bloch waves which we will denote $|\psi_{\mathbf{k}}\rangle$ because the

good quantum number is the momentum $\mathbf{k}$ (as the system is invariant under translations by primitive lattice vectors of the lattice of MUC's). Similar to the regular Bloch theorem we then have then achieved the magnetic Bloch theorem:

$$(T_x^M)^q \left|\psi_{\mathbf{k}}\right\rangle = e^{iqk_x a} \left|\psi_{\mathbf{k}}\right\rangle \quad T_y^M \left|\psi_{\mathbf{k}}\right\rangle = e^{ik_y a} \left|\psi_{\mathbf{k}}\right\rangle, \tag{3.32}$$

where $0 < k_x \leq \frac{2\pi}{qa}$ and $0 < k_y \leq \frac{2\pi}{a}$.

3.2.1. Hofstadter's butterfly

As a way of checking whether the Peierls phases and periodic boundary conditions in the presence of a magnetic field have been applied correctly in the numerical calculations, we have reproduced Hofstadter's butterfly. This is the fractal pattern formed by the energy spectrum of a 2D square lattice with nearest-neighbor hopping as a function of the magnetic flux. The pattern arises due to the energy levels being affected both by the periodic potential of the lattice and the perpendicular magnetic field. Hence there are two competing length scales of the system; the lattice constant a and the magnetic length $l_B = \sqrt{\frac{\hbar}{eB}}$. In order for Hofstadter's butterfly to emerge, the two length scales must be commensurate, which is only the case for rational flux per plaquette [12]

$$\Phi = \frac{a^2 B}{\Phi_0} = \frac{p}{q}, \tag{3.33}$$

where p and q are coprime integers. See fig. 3.2 for Hofstadter's butterfly in the case of nearest-neighbor hopping in a square lattice of size 20×20, where the energy spectrum is calculated for different rational fluxes Φ between 0 and 1.
Hofstadter's butterfly for systems with next-nearest neighbor hopping has also been studied previously by Hatsugai and Kohmoto [13] and we have similarly reproduced these results. This is seen in fig. 3.3.

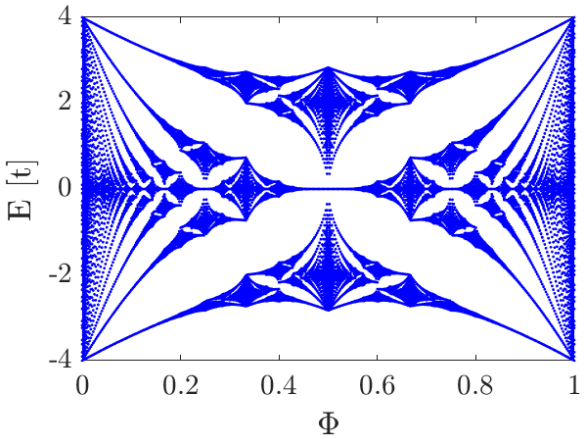

Figure 3.2.: Hofstadter's butterfly for nearest-neighbor hopping $t = 1$

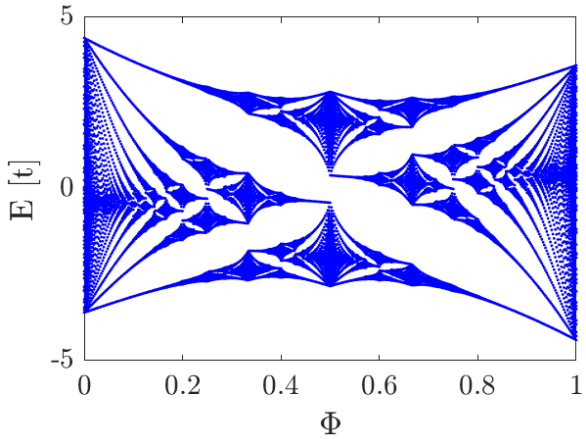

Figure 3.3.: Hofstadter's butterfly for nearest and next-nearest neighbor hopping $t = 1, t' = -0.1$

3.2.2. The magnetic Bloch theorem for superconductors

It is now investigated how the magnetic Bloch theorem is constructed in the specific case of a superconductor. When a magnetic field $H_{c_1} < H < H_{c_2}$ is applied to a superconductor the magnetic field penetrates the material and an Abrikosov vortex lattice forms. H_{c_1} and H_{c_2} are the lower and upper critical fields respectively. Each vortex is penetrated by one superconducting flux quantum $\Phi_0^{SC} = \frac{h}{2e}$ [4].

This means that the strength of the magnetic field and the size of the MUC must be adjusted so that each MUC is penetrated by two superconducting flux quanta and contains two vortices. In the following we will use the notation

$$\mathcal{T}_{mn} = \left(T_x^M\right)^{mN_x} \left(T_y^M\right)^{nN_y}, \tag{3.34}$$

for a general magnetic translation operator which translates by m magnetic unit cells in the x-direction and n in the y-direction. That is, the MTO translates a vector $\mathbf{r}$ according to

$$\mathcal{T}_{mn}\mathbf{r} = \mathbf{r} + \mathbf{R}, \tag{3.35}$$

where $\mathbf{R} = mN_x\hat{e}_x + nN_y\hat{e}_y$ is a lattice vector of the lattice of magnetic unit cells. This applies in our case where the underlying lattice is a 2D square lattice.
We still consider a uniform B-field pointing in the direction of $\hat{e}_z$, and use the Landau gauge $\mathbf{A} = (-By, 0, 0)$. We will now figure out how the superconducting order parameter transforms under a translation $\mathcal{T}_{mn}$ as defined above. In order to do that, we firstly examine how the vector potential transforms. The translation can be split up into separate translations in the x- and y-direction:

$$\mathcal{T}_{mn} = \mathcal{T}_{0n}\mathcal{T}_{m0}. \tag{3.36}$$

Since the magnetic field is chosen to be uniform, a translation can only modify the vector potential by the gradient of a scalar field. For a translation in the x-direction we get:

$$\begin{aligned} \mathcal{T}_{m0}A(\mathbf{r}) = A(\mathbf{r}) &= A(\mathbf{r}) + \nabla\phi_1 \\ &\implies \phi_1 = \text{constant}. \end{aligned} \tag{3.37}$$

Without loss of generality we can choose $\phi_1 = 0$. Correspondingly a translation in the y-direction yields:

$$\begin{aligned} \mathcal{T}_{0n}\mathbf{A}(\mathbf{r}) = -B(y + nN_y a)\hat{x} &= \mathbf{A}(\mathbf{r}) + \nabla\phi_2 \\ \implies \phi_2 &= -BnN_y a x. \end{aligned} \tag{3.38}$$

It is also necessary to consider how the superconducting order parameter transforms under such a translation. Since $\Delta_i = V\langle c_{i\downarrow}c_{i\uparrow}\rangle$, we can find the transformation properties of Δ_i if we know those of the $c_{i\sigma}$-operators. As seen above the translation corresponds to a gauge transformation of the vector potential. The on-site creation and annihilation operators transform like the wave function under a gauge transformation [8], so:

$$\begin{aligned} & c_{i\sigma} \to c_{i\sigma}e^{-i\frac{e}{\hbar}\Lambda(\mathbf{r}+\mathbf{R})} \\ \implies & c_{i\sigma} \to c_{i\sigma}e^{-i\frac{2\pi}{\Phi_0}(\phi_1(\mathbf{r}+\mathbf{R})+\phi_2(\mathbf{r}+\mathbf{R}))} = c_{i\sigma}e^{-i\frac{2\pi}{\Phi_0}(0-BnN_y a(x+mN_x a))}. \end{aligned} \tag{3.39}$$

Hence

$$\begin{aligned} \Delta(\mathcal{T}_{mn}\mathbf{r}) &= e^{-i\frac{4\pi}{\Phi_0}\cdot 0}e^{-i\frac{4\pi}{\Phi_0}(-BN_y a(x+mN_x a))}\Delta(\mathbf{r}) \\ &= e^{i\chi(\mathbf{r},\mathbf{R})}\Delta(\mathbf{r}), \end{aligned} \tag{3.40}$$

$$\begin{aligned} \chi(\mathbf{r},\mathbf{R}) &\equiv -\frac{4\pi}{\Phi_0}(-BnN_y a(x + mN_x a)) \\ &= -\frac{4\pi}{\Phi_0}\mathbf{A}(\mathbf{R})\cdot\mathbf{r} + 4\pi mn. \end{aligned} \tag{3.41}$$

It was invoked that $N_x N_y a^2 B = \Phi_0$ (which corresponds to the condition of a magnetic flux of two

superconducting flux quanta through each magnetic unit cell). We might as well define

$$\chi(\mathbf{r},\mathbf{R}) \equiv -\frac{4\pi}{\Phi_0}\mathbf{A}(\mathbf{R})\cdot\mathbf{r}, \tag{3.42}$$

since $e^{-i4\pi mn} = 1$ for m, n integers. It now only remains to formulate the magnetic Bloch theorem for the Bogoliubov wave function $\psi(\mathbf{r}) = \begin{pmatrix} u(\mathbf{r}) \\ v(\mathbf{r}) \end{pmatrix}$. In order to do this we construct a translation operator for this wave function which is given by [11]

$$\mathcal{T}_{mn}\psi(\mathbf{r}) = \begin{pmatrix} e^{i\chi(\mathbf{r},\mathbf{R})/2} & 0 \\ 0 & e^{-i\chi(\mathbf{r},\mathbf{R})/2} \end{pmatrix} \begin{pmatrix} u(\mathbf{r}-\mathbf{R}) \\ v(\mathbf{r}-\mathbf{R}) \end{pmatrix}. \tag{3.43}$$

This ensures that the superconducting order parameter transforms correctly, since it gets its complex phase from the product $u_{i,l}v^*_{i,l}$ (see eq. 2.32). The reason for choosing this transformation of the eigenstates is that we still need the translation operator to commute with the Bogoliubov-de Gennes Hamiltonian in eq. 2.30, which is ensured by this particular choice. In accordance with the result from the previous section (see eq. 3.32) we can now formulate the magnetic Bloch theorem for the BdG-wavefunction. It is completely similar, except that there is an extra phase as is seen from the above calculations. Hence:

$$\begin{pmatrix} u(\mathbf{r}+\mathbf{R}) \\ v(\mathbf{r}+\mathbf{R}) \end{pmatrix} = e^{i\mathbf{k}\cdot\mathbf{R}} \begin{pmatrix} e^{i\chi(\mathbf{r},\mathbf{R})/2}u(\mathbf{r}) \\ e^{-i\chi(\mathbf{r},\mathbf{R})/2}v(\mathbf{r}) \end{pmatrix}, \tag{3.44}$$

where

$$\mathbf{k} = \frac{2\pi l_x}{M_x N_x}\hat{e}_x + \frac{2\pi l_y}{M_y N_y}\hat{e}_y, \quad l_i = 0, 1, ..., M_i - 1, \quad i = \{x, y\}.$$

N_x and N_y are the number of sites in x- and y-direction of the MUC respectively. M_x and M_y is the number of MUC's in each direction.

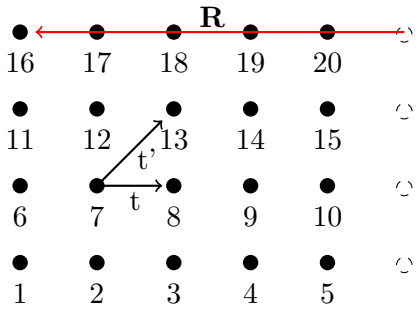

Figure 3.4.: Illustration of a MUC with $N_x = 5$ and $N_y = 4$. Periodic boundary conditions are applied so that e.g. a particle which tunnels to the right from site 20 is translated by $\mathbf{R}$ to site 16 and acquires a complex phase.

This result allows us to use periodic boundary conditions in the numerical calculations, as long as we take these extra phases into account. An electron tunneling to a point which is not in the magnetic unit cell is translated to the other side of the system by the vector $\mathbf{R}$ and acquires a phase given by eq. 3.44. See fig. 3.4.

The magnetic Bloch theorem also enables the use of the so-called Supercell method, which utilizes that eq. 3.44 block diagonalizes the Hamiltonian of eq. 2.30, so that the numerical calculations can be carried out $M_x \times M_y$ times for matrices of size $2N_x \times 2N_y$ instead of one matrix of dimension $2N_xM_x \times 2N_yM_y$. This significantly improves the size of the systems which it is possible to solve the Bogoliubov-de Gennes equations numerically for. For further details on this method see [14].

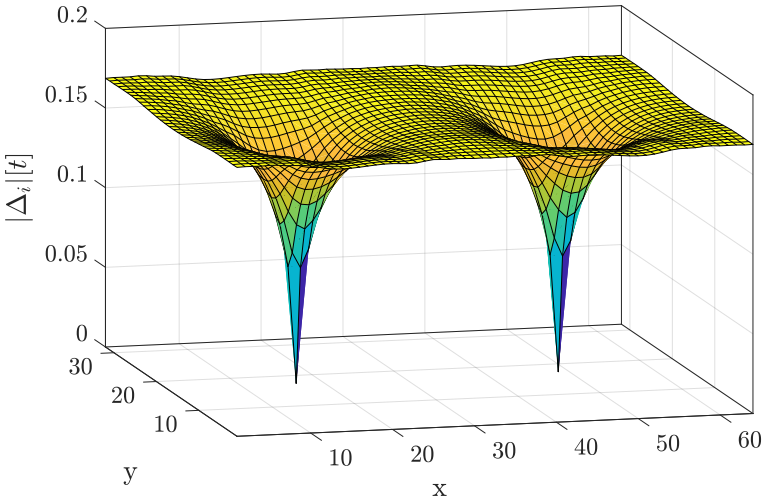

Figure 4.1.: Vortices in a system of dimension 64×32 with nearest- and next-nearest neighbor hopping. The parameters used are $t = 1$, $t' = -0.15t$, $V = -1.95t$ and the temperature is $k_B T = 0.01$. The magnetic field strength is adjusted so that two half flux quanta $\Phi_0 = \frac{h}{2e}$ penetrate the system

4. Numerical calculations

4.1. Vortices

In order to figure out how vortices are created in a specific superconducting system which is subject to a nonzero magnetic field, the Bogoliubov-de Gennes equations are solved numerically. We consider the case of a square lattice with a B-field in the $\hat{e}_z$-direction. In order to simplify the Peierls phases which arise from the vector potential, we choose the Landau gauge $\mathbf{A} = (-By, 0, 0)$. We apply periodic boundary conditions according to the principles presented in the previous section. The sites in the lattice are numbered linearly starting from the lower left corner of the lattice and ending in the upper right corner (cf. fig. 3.4). There are $Nx \times Ny$ sites in the lattice. The matrix in eq. 2.30, which has dimension $2NxNy \times 2NxNy$, is then constructed and diagonalized numerically. The coupling constant V is chosen so that $\Delta_i \ll t$. For each eigenvalue we then get an eigenvector containing u_n and V_n on each site, allowing us the calculate the on-site order parameter Δ_i according to eq. 2.32. The matrix is then updated using the new Δ_i's. This procedure is repeated until the result is self-consistent. Then other quantities such as the density of particles at each site and the supercurrents in the system can be calculated using the self-consistent eigenvalues and eigenvectors of the system. When the Bogoliubov-de Gennes equations are solved numerically according to this method, vortices appear as is seen in fig. 4.1.

4.1.1. Coherence length

The coherence length ξ of the superconductor is a measure of the size of the Cooper pairs. It is the characteristic length scale at which the SCOP regains its bulk value when suppressed at the vortex core. Hence the width of the vortex is 2ξ. It is a result from microscopic BCS theory that the superconducting coherence length can be estimated by [4]

$$\xi = \frac{\hbar v_F}{\Delta \pi}, \tag{4.1}$$

where v_F is the Fermi velocity which has to be calculated for the present case of a 2D square lattice in the tight-binding model. This result can be used to check whether the numerical results from the simulation are sensible. Furthermore it serves as a measure of figuring out suitable values for the chemical potential

and the coupling constant (which determine the magnitude of the superconducting order parameter), so that the system is large enough to contain two vortices. The Fermi velocity is given by

$$v_F = \frac{1}{\hbar}\frac{\partial \varepsilon}{\partial \mathbf{k}}\Big|_{k=k_F}, \tag{4.2}$$

where in our case the dispersion relation is [5]

$$\varepsilon(\mathbf{k}) = -2t\left[\cos(k_x a) + \cos(k_y a)\right] - 4t' \cos(k_x a)\cos(k_y a) - \mu. \tag{4.3}$$

We are at low temperatures ($k_B T < 0.1t$) so $E_F \simeq \mu$. We choose the chemical potential so that the Fermi surface is approximately circular and $k_{F,x} \simeq k_{F,y} \simeq \frac{1}{\sqrt{2}} k_F$. Combining eqs. 4.2 and 4.3 yields:

$$v_F = \frac{4ta}{\hbar}\sin\left(\frac{a}{\sqrt{2}}k_F\right) + \frac{8t'a}{\hbar}\cos\left(\frac{a}{\sqrt{2}}k_F\right)\sin\left(\frac{a}{\sqrt{2}}k_F\right). \tag{4.4}$$

The Fermi wave vector can be determined from

$$E_F = \varepsilon(\mathbf{k}_F) = -4t\cos\left(\frac{1}{\sqrt{2}}k_F a\right) - 4t'\cos^2\left(\frac{1}{\sqrt{2}}k_F a\right) - \mu \simeq \mu. \tag{4.5}$$

Solving eq. 4.5 provides us with a value of k_F and the coherence length is then:

$$\xi = \frac{4a}{\Delta\pi}\sin\left(\frac{a}{\sqrt{2}}k_F\right)\left(t + 2t'\cos\left(\frac{a}{\sqrt{2}}k_F\right)\right). \tag{4.6}$$

When using the parameters $t = 1, t' = -0.15$ and $\mu = 0.6$, resulting in a bulk value of the SCOP of $\Delta = 0.17t$, which are the parameters used in fig. 4.1, we get the coherence length $\xi \simeq 8a$. This is consistent with what is obtained from the numerical calculations (the width of the vortex is approximately $2\xi \simeq 16a$. As the coupling constant V determines the bulk value of the SCOP, it is also possible to figure out what the smallest possible value of V is for a given system size in order for it to contain two vortices. This confirms what has been found from the numerical calculations: namely that with a system size of 64×32, $\mu = 0$ and $t' = -0.2$, the minimum value is approximately $V = -1.5t$ which gives a SCOP bulk value of $\Delta = 0.07t$ and coherence length $\xi \simeq 17a$. It has been found that at this value the system is large enough to contain two vortices, but the SCOP does not completely reach its bulk value between them.

4.2. Supercurrents

When the magnetic field penetrates the superconductor and vortices are created, a current is also generated in the material. We investigate how this supercurrent runs in the material. An expression for the total current on a site in the lattice can be found from the continuity equation:

$$\frac{\partial \hat{\rho}_i}{\partial t} + \left(\nabla \cdot \hat{\mathbf{j}}\right)_i = 0, \tag{4.7}$$

where $\hat{\rho}_i = -e\hat{n}_i$. We calculate the time derivative of the particle density operator which is given by [8]:

$$\dot{\hat{n}}_i = \frac{i}{\hbar}\left[H_{BCS}, \hat{n}_i\right]. \tag{4.8}$$

The commutators of each of the three terms of the Hamiltonian in eq. 2.20 with the number operator $\hat{n}_i = \sum_\sigma c^\dagger_{i\sigma} c_{i\sigma}$ are now determined. $[H_2, \hat{n}_i]$ is trivially zero, since the number operator of course

commutes with itself. Using the standard anticommutation relations we also easily obtain:

$$[H_3, \hat{n}_j] = -V \sum_{i\sigma} \left[c^\dagger_{i\uparrow} c_{i\uparrow} c^\dagger_{i\downarrow} c_{i\downarrow}, c^\dagger_{j\sigma} c_{j\sigma} \right] = 0. \tag{4.9}$$

Had we used the mean-field BCS Hamiltonian, this term would not have been zero because there is no conservation of particles in the mean-field BCS theory. Naturally this does not reflect the real physical situation.

Hence, the only nonzero term is the commutator of the first term with the density operator. Again, using anticommutation relations as well as commutator and anticommutator identities we find:

$$[H_1, \hat{n}_k] = \sum_{ij\sigma\sigma'} t_{ij} \left[e^{i\phi_{ij}} c^\dagger_{i\sigma} c_{j\sigma}, c^\dagger_{k\sigma'} c_{k\sigma'} \right] = \sum_{j\sigma} \left[t_{jk} e^{i\phi_{jk}} c^\dagger_{j\sigma} c_{k\sigma} - t_{kj} e^{i\phi_{kj}} c^\dagger_{k\sigma} c_{j\sigma} \right]. \tag{4.10}$$

Then eq. 4.7 becomes

$$\left(\nabla \cdot \hat{\mathbf{j}} \right)_i = -\frac{\partial \hat{\rho}_i}{\partial t} = e\dot{\hat{n}}_i = \frac{ie}{\hbar} \sum_{j\sigma} \left(t_{ji} e^{i\phi_{ji}} c^\dagger_{j\sigma} c_{i\sigma} - t_{ij} e^{i\phi_{ij}} c^\dagger_{i\sigma} c_{j\sigma} \right), \tag{4.11}$$

where we get a contribution from nearest and next-nearest neighbors. But each term j is just the difference between the charge moving from site i to site j and the charge moving from site j to site i. Thus each term j is the net current running from site i to site j. That is,

$$\left(\nabla \cdot \hat{\mathbf{j}} \right)_i = \sum_j j_{i\to j}. \tag{4.12}$$

We calculate the expectation value of each term j and perform the Bogoliubov-de Gennes transformation in eq. 2.23, and using the correspondence between positive and negative eigenvalues we find that the total current between sites i and j is given by (see appendix G for the detailed calculations):

$$\begin{aligned} \langle j_{i\to j} \rangle = \frac{ie}{\hbar} \sum_l & \left[t_{ji} e^{i\phi_{ji}} u^*_{l,j\uparrow} u_{l,i\uparrow} - t_{ij} e^{i\phi_{ij}} u^*_{l,i\uparrow} u_{l,j\uparrow} \right] f(E_{l\uparrow}) \\ + \sum_l & \left[t_{ji} e^{i\phi_{ji}} v^*_{l,i\downarrow} v_{l,j\downarrow} - t_{ij} e^{i\phi_{ij}} v_{l,i\downarrow} v^*_{l,j\downarrow} \right] f(-E_{l\uparrow}). \end{aligned} \tag{4.13}$$

The sum is over both positive and negative eigenvalues. There are non-zero terms for nearest and next-nearest neighbors with $t_{ij} = t_{ji}$ equal to t and t' respectively. The total current on a site is then a vector which can be found by summing over the currents to the four nearest-neighbors and four next-nearest neighbors:

$$\langle j_i \rangle = \sum_{\langle i,j \rangle} \langle j_{i\to j} \rangle + \sum_{\langle\langle i,j \rangle\rangle} \langle j_{j_i \to j} \rangle, \tag{4.14}$$

where $\langle i,j \rangle$ and $\langle\langle i,j \rangle\rangle$ denote that the sums are over nearest and next-nearest neighbors respectively. By performing this calculation using the self-consistent eigenvectors obtained from the numerical solution of the BdG-equations, we find the supercurrents, which are readily seen to be circulating the vortices. This is seen in fig. 4.2 (for the system in fig. 4.1).

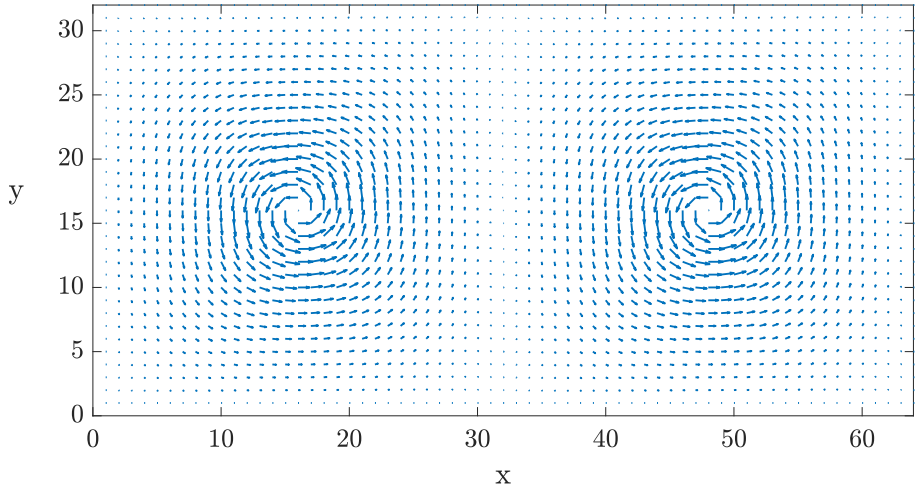

Figure 4.2.: Plot of current vectors at each site of the lattice in units of $\left[\frac{et}{\hbar}\right]$. A plot of the SCOP for this system is seen in fig. 4.1. The supercurrents are circulating the vortex cores.

4.3. Numerically determining the presence of vortices

When impurities are introduced in the superconductor, it is no longer possible to locate the vortices by investigating the plot of the superconducting order parameter and looking for nodal points of the SCOP, as the order parameter is also suppressed on impurity sites. Thus another method which enables us to determine whether there are vortices in the system is necessary. This can be done by considering the complex phase of the SCOP. We can write $\Delta_i = |\Delta_i| e^{i\theta_i}$, where θ_i is the phase at site i. The phase then forms a two-dimensional scalar field and has a singularity at the center of the vortex where it is undefined. Furthermore, in order for the phase to be defined everywhere else (single-valued) the total change of the phase along any closed path enclosing the vortex must be equal to $2\pi n$ [15]. This property can be used to determine whether the system contains vortices. We choose a closed path and calculate the total phase change along this path. If the result is $\pm 2\pi$ a vortex is enclosed by the path. The phase lies in the interval $-\pi < \theta \leq \pi$ but is also periodic which means that $-\pi$ and π are the same phase. There are always two possible choices for the difference between two phases: $\Delta\theta_i = \theta_{i+1} - \theta_i$ and $\Delta\theta_i' = \Delta\theta_i - 2\pi$.

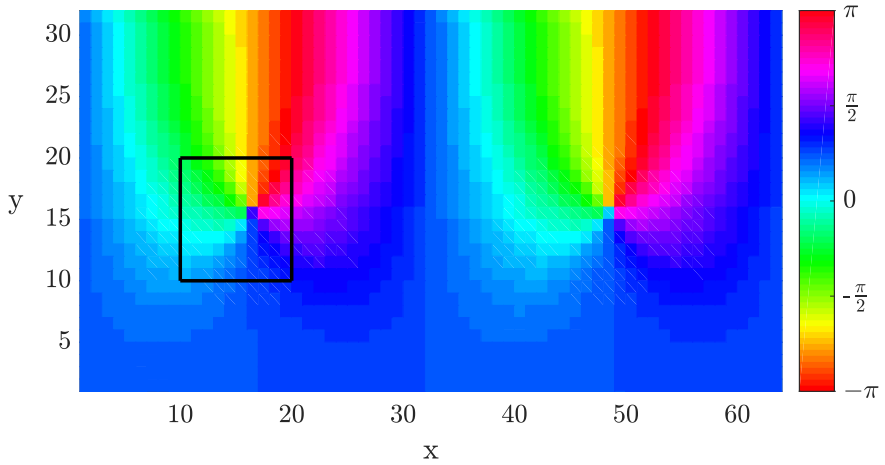

Figure 4.3.: The complex phase of the SCOP in a system with two vortices. The total phase change when going counter-clockwise around the black path to the left is -2π, which confirms that a vortex is enclosed by this path. The singularity of the phase which is the location of the vortex is also visible as the point where all phases meet.

Due to this ambiguity we need to unwrap the phase so that if the jump between two points is larger than π we subtract 2π and use this completely equivalent difference instead. In fig. 4.3 a plot of the complex phase of the SCOP in the system in fig 4.1 is seen. Furthermore a path which yields a total phase change of -2π when going counterclockwise is shown in black, confirming that a vortex is enclosed. From the plot one can also approximately determine the position of the vortices as the singular points where all phases meet. This method allows for determining whether vortices are present even if this is not visible from the plot of the magnitude of the SCOP. Furthermore the circulating supercurrents indicate that vortices are present and suggest their location, serving as a way of confirming the results found using the phase.

5. Impurities

As found by [1], the critical temperature of an s-wave superconductor can be enhanced in the presence of impurities. This happens because impurities cause regions of reinforced density of states. However, in this case it is not self-evident what should be defined as the critical temperature, since the superconductivity is not destroyed everywhere in the superconductor at once. Instead some regions remain superconducting while others are in the normal state. But if vortices are sustained in the system we know that $T < T_c$. Hence, using the method described in section 4.3, we seek to reproduce this effect of T_c-enhancement. If vortices are found in the presence of impurities above the critical temperature for the homogeneous system (T_c^0) we can confirm that the critical temperature is enhanced by the impurities.
Of course it would have been desirable to use the same parameters in the numerical calculations as was used by [1] ($V = -0.8t, t = 1, t' = -0.3$). However, as was found in section 4.1.1 the smallest possible coupling constant for a system of size 64×32 is $V = -1.5t$, so this value has been used along with the hopping constants $t = 1$ and $t' = -0.2$. For this system the critical temperature without impurities is $k_B T_c^0 = 0.06$. We now investigate whether vortices can be detected at $k_B T = 0.07$ when impurities of strength $V^{\text{imp}} = 10t$ are distributed randomly on 15 % of the lattice sites. For comparison the numerical calculations have been carried out at lower temperatures ($k_B T = 0.02$ and $k_B T = 0.055$) as well. A real-space plot of $\frac{|\Delta_i|}{\Delta_0}$ at $k_B T = 0.07$ with impurities is seen in fig 5.1. $\Delta_0 = 0.0985$ is the magnitude of the SCOP for the homogeneous system at $k_B T = 0$. It is seen that connected regions of nonzero Δ emerge above T_c^0 in the presence of impurities.

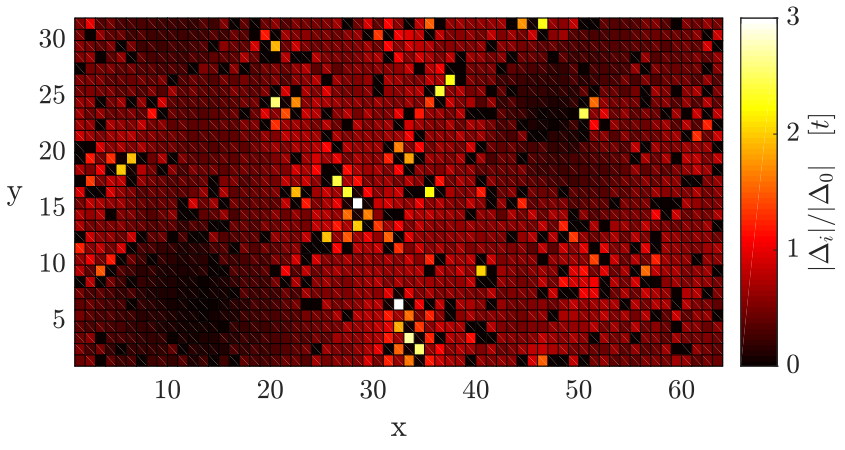

Figure 5.1.: Absolute value of the SCOP at each cite. Large fluctuations are seen due to the presence of impurities. Though $|\Delta|$ appears to be somewhat more suppressed in some regions, it is no longer obvious whether vortices are present. Connected regions of nonzero $|\Delta|$ are also observed.

This indicates that the critical temperature has been increased. When a magnetic field is applied and the total change of the complex phase of the SCOP is calculated along the borders of each quadratic half of the system, this yields the value -2π. A plot of the complex phase at $k_BT = 0.07$ and at $k_BT = 0.02$ is seen in appendix H (fig. H.1) and as was the case for the homogeneous system it is possible from this to approximately determine the location of the vortices as the singular points where all phases meet. Furthermore the supercurrents are calculated also in this case, and we see that they are circulating the points where the phase plot showed singularities. This is also seen in appendix H (fig. H.2). At all three temperatures the average magnitude of the current vectors and the SCOP are calculated. These results are seen in table 5.1, and both quantities decrease with increasing temperature but are nonzero even above T_c^0. Hence it is confirmed that vortices are present in the system above T_c^0.

k_BT $[t]$	$\lvert j_i\rvert_{av} = \frac{1}{N_xN_y}\sum_i \lvert j_i\rvert$ $\left[\frac{et}{\hbar}\right]$	$\lvert\Delta_i\rvert_{av} = \frac{1}{N_xN_y}\sum_i \lvert\Delta_i\rvert$ $[t]$
0.02	$4.5 \cdot 10^{-3}$	0.10
0.055	$1.6 \cdot 10^{-3}$	0.077
0.07	$5.2 \cdot 10^{-4}$	0.049

Table 5.1.: Average magnitude of the supercurrents and the SCOP for different temperatures below and above $k_BT_c = 0.06$ in a system with 15% impurities. Both quantities decrease with increasing temperature but are non-zero even above the critical temperature ($k_BT = 0.07$)

We have also investigated whether the results are consistent with what is found by previous studies by applying the definition of the critical temperature used by [1] to the present case. That is, we choose some threshold p, and define T_c as the highest temperature where all edges are still connected by regions of $|\Delta_i| > p\Delta_0$. At $k_BT = 0.07$ we find that for the values of p used by [1] (0.02, 0.05 and 0.10), all edges are connected. Plots depicting these results are seen in appendix H, fig. H.3. This is also the case when considering the same system but without a magnetic field. For the system with no magnetic field the edges are connected for all $p \leq 0.45$, and with a magnetic field for $p \leq 0.4$. Hence we have reproduced the results found by Andersen and Gastiasoro in [1], namely that T_c has been increased due to the presence of impurities. This is the conclusion no matter which of the two definitions of the critical temperature is used.

6. Conclusion

It has been investigated how applying a magnetic field to an s-wave superconductor causes vortices to emerge. This has been done by solving the Bogoliubov-de Gennes equations numerically in the tight-binding model with periodic boundary conditions. Prior to this, studies of the Peierls substitution which modifies the hopping constant in the presence of a magnetic field and the magnetic Bloch theorem, which enables the use of periodic boundary conditions have been conducted. The presence of vortices has been determined by considering the complex phase of the SCOP. When summing the phase differences along a closed path one gets the value $2\pi n$ if a vortex is enclosed by the path. This method has proven useful even in the case of an inhomogeneous system with impurities. Hence we have shown that vortices are present above the critical temperature in the presence of impurities on 15% of the lattice sites. This conclusion is further supported by the fact that supercurrents are circulating the regions containing vortices, and by considering the real-space plot of $|\Delta_i|$ which shows regions where the SCOP is nonzero. All edges are also still connected by regions where the SCOP satisfy that $|\Delta_i| > p\Delta_0$, so this definition of T_c is also

satisfied. That is, the effect of T_c-enhancement caused by impurities found by [1] has been reproduced for a system of size 64×32 with $V = -1.5t$, $t = 1\, t' = -0.2$ and $V^{\text{imp}} = 10t$. Were this study to be pursued further, one could consider larger systems thus enabling the use of the same parameters as was used by [1]. By repeating the numerical calculations multiple times at different temperatures it would also be possible to determine the critical temperature in a system with impurities. One option is to combine the definitions of T_c from this thesis (vortices are sustained) and [1] (edges are connected by regions of $|\Delta_i| > p\Delta_0$). One could also determine the temperature where vortices are no longer sustained, and use this result to figure out which value of p should be employed in the definition of T_c from [1] in order for these two methods to be consistent.

Bibliography

[1] Maria N. Gastiasoro, Brian M. Andersen, Enhancing Superconductivity by Disorder, December 8, 2017, arXiv:1712.02656v1 [cond-mat.supr-con]

[2] Henrik Bruus, Karsten Flensberg, Many-Body Quantum Theory in Condensed Matter Physics, Oxford University Press, 2007

[3] James F. Annett, Superconductivity, Superfluids and Condensates, Oxford University Press 2011

[4] Brian Møller Andersen, lecture notes for the course Condensed Matter Physics 2, Niels Bohr Institute, 2018

[5] Carl J. Chandler, Christian Prosko & F. Marsiglio, The Effect of Next-Nearest Neighbor Hopping in the One, Two, and Three Dimensional Holstein Model, Nature Scientific Reports, 2/9 2016

[6] Stephen Blundell, Magnetism in Condensed Matter, Oxford University Press 2014

[7] Jian-Xin Zhu, Bogoliubov de-Gennes Method and Its Applications, Springer Lecture Notes in Physics Volume 924

[8] J. J. Sakurai, Modern Quantum Mechanics Revised Edition, Addison-Wesley Publishing Company, 1994

[9] Steve Simon, The Oxford Solid State Basics, Oxford, 2016

[10] Monika Aidelsburger, Artificial Gauge Fields with Ultracold Atoms in Optical Lattices, Chapter 2: Square Lattice with Magnetic Field, Dissertation, München 2015

[11] Benat Mencia Uranga, Vortices in Unconventional Correlated Superconductors, Master Thesis, Niels Bohr Institute, 2014

[12] Gustav M. Obermair, Bloch Electrons in Rational and Irrational Magnetic Fields, Helvetica Physica Acta, 56 1983

[13] Y. Hatsugai and M. Kohmoto, Energy spectrum and the Quantum Hall Effect on the Square Lattice with Next-nearest-neighbor Hopping, Physical Review B, Volume 42, Number 13, 1 November 1990

[14] Markus Schmid, Brian M. Andersen, Arno P. Kampf and P. J. Hirschfeld, d-Wave Superconductivity as a Catalyst for Antiferromagnetism in Underdoped Cuprates, New Journal of Physics, 2010 **12** 053043

[15] Alexander John Taylor, Analysis of Quantised Vortex Tangle, Springer Theses 2017

Appendix A: BCS theory

In this section the analytical derivation of the superconducting order parameter for a homogeneous system at zero temperature, and an expression for the critical temperature is presented. Considering the self-consistency equation:

$$\Delta = V \sum_{\mathbf{k}} \frac{\Delta}{2E_{\mathbf{k}}} \tanh\left(\frac{E_{\mathbf{k}}}{2k_B T}\right), \tag{A.1}$$

we rewrite the sum over k-states to an integral with respect to energy:

$$\begin{aligned} \Delta &= VN(0) \int_0^{\hbar\omega_D} d\varepsilon \frac{\Delta}{2E_{\mathbf{k}}} \tanh\left(\frac{E_{\mathbf{k}}}{2k_B T}\right) \\ \implies 1 &= VN(0) \int_0^{\hbar\omega_D} d\varepsilon \frac{1}{2E_{\mathbf{k}}} \tanh\left(\frac{E_{\mathbf{k}}}{2k_B T}\right), \\ &\text{where} \quad E_{\mathbf{k}} = \sqrt{\varepsilon^2 + |\Delta|^2}. \end{aligned} \tag{A.2}$$

$N(0)$ is the density of states at the Fermi level, and this has been taken outside the integral, as we assume that it only varies little in the interval of integration. Since $\tanh\left(\frac{1}{x}\right) \to 1$ for $x \to 0$, at $k_B T = 0$ we obtain

$$1 = VN(0) \int_0^{\hbar\omega_D} d\varepsilon \frac{1}{2\sqrt{\varepsilon^2 + \Delta^2}} = \frac{VN(0)}{2} \sinh^{-1}\left(\frac{\hbar\omega_D}{\Delta}\right). \tag{A.3}$$

And in the weak-coupling limit $VN(0) << 1$ we can solve for Δ to get:

$$\Delta(0) = 2\hbar\omega_D \exp\left(\frac{-2}{VN(0)}\right), \tag{A.4}$$

At the critical temperature T_c where the superconducting order parameter vanishes we have no Cooper pairs so $\Delta = 0$. This means that $E \to \varepsilon$ so that eq. A.2 becomes

$$1 = \frac{VN(0)}{2} \int_0^{\hbar\omega_D} d\varepsilon \frac{1}{\varepsilon} \tanh\left(\frac{\varepsilon}{2k_B T_c}\right). \tag{A.5}$$

By changing variable to $x \equiv \frac{\varepsilon}{2k_B T_c}$ and using integration by parts, the integral in eq. A.5 can be carried out and an expression for the critical temperature T_c can be found. The critical temperature is the temperature where the superconducting order parameter vanishes. In the weak-coupling limit it is:

$$k_B T_c = 1.13\hbar\omega_D \exp\left(-\frac{2}{N(0)V}\right). \tag{A.6}$$

Appendix B: Commutators

In this section the commutators of each of the terms in the mean-field BCS Hamiltonian (see eq. 2.20) with the creation and annihilation operators are calculated. This is done using the anticommutator relations for the fermion creation and annihilation operators: Considering the first term we get:

$$\begin{aligned}
[H_1, c_{i\uparrow}] &= -\sum_{ij\sigma} t_{ij} \left[c^\dagger_{i\sigma} c_{j\sigma}, c_{i\uparrow} \right] \\
&= -\sum_{j\sigma} t_{ij} \left(c^\dagger_{i\sigma} \{c_{j\sigma}, c_{i\uparrow}\} - \{c^\dagger_{i\sigma}, c_{i\uparrow}\} c_{j\sigma} \right) \\
&= \sum_{j\sigma} t_{ij} \delta_{\sigma\uparrow} c_{j\sigma} \\
&= \sum_{j} t_{ij} c_{j\uparrow}.
\end{aligned} \tag{B.1}$$

Similarly

$$[H_1, c_{i\downarrow}] = \sum_{j} t_{ij} c_{j\downarrow}. \tag{B.2}$$

The second term in the Hamiltonian yields

$$\begin{aligned}
[H_2, c_{i\uparrow}] &= \sum_{i\sigma} (V^{\text{imp}}_{i\sigma} - \mu) \left[c^\dagger_{i\sigma} c_{i\sigma}, c_{i\uparrow} \right] \\
&= \sum_{\sigma} (V^{\text{imp}}_{i\sigma} - \mu) \left(c^\dagger_{i\sigma} \{c_{i\sigma}, c_{i\uparrow}\} - \{c^\dagger_{i\sigma}, c_{i\uparrow}\} c_{i\sigma} \right) \\
&= -\sum_{\sigma} (V^{\text{imp}}_{i\sigma} - \mu) \delta_{\sigma\uparrow} c_{i\sigma} \\
&= -(V^{\text{imp}}_{i\uparrow} - \mu) c_{i\uparrow}.
\end{aligned} \tag{B.3}$$

And:

$$[H_2, c_{i\downarrow}] = -(V^{\text{imp}} - \mu) c_{i\downarrow}. \tag{B.4}$$

Finally we have:

$$\begin{aligned}
[H_3, c_{i\uparrow}] &= -\sum_{i} \left(\Delta^*_i [c_{i\downarrow} c_{i\uparrow}, c_{i\uparrow}] + \Delta_i [c^\dagger_{i\uparrow} c^\dagger_{i\downarrow}, c_{i\uparrow}] \right) \\
&= -\left(\Delta^*_i (c_{i\downarrow} \{c_{i\uparrow}, c_{i\uparrow}\} - \{c_{i\downarrow}, c_{i\uparrow}\} c_{i\uparrow}) + \Delta_i (c_{i\uparrow} \{c^\dagger_{i\downarrow}, c_{i\uparrow}\} - \{c^\dagger_{i\uparrow}, c_{i\uparrow}\} c^\dagger_{i\downarrow}) \right) \\
&= \Delta_i c^\dagger_{i\downarrow}.
\end{aligned} \tag{B.5}$$

And:

$$[H_3, c_{i\downarrow}] = -\Delta_i c^\dagger_{i\uparrow}. \tag{B.6}$$

By combining these three expressions we finally get

$$\begin{aligned}[H, c_{i\uparrow}] &= \sum_j t_{ij} c_{j\uparrow} - (V_{i\uparrow}^{\text{imp}} - \mu) c_{i\uparrow} + \Delta_i c_{i\downarrow}^\dagger, \\ [H, c_{i\downarrow}] &= \sum_j t_{ij} c_{j\downarrow} - (V_{i\downarrow}^{\text{imp}} - \mu) c_{i\downarrow} - \Delta_i c_{i\uparrow}^\dagger.\end{aligned} \tag{B.7}$$

Appendix C: Bogoliubov-de Gennes equations

The Bogoliubov-de Gennes equations are:

$$\begin{pmatrix} \hat{h_\uparrow} & -\Delta_i \\ -\Delta_i^* & -\hat{h_\downarrow}^* \end{pmatrix} \begin{pmatrix} u_{n\uparrow} \\ v_{n\downarrow} \end{pmatrix} = E_{n\uparrow} \begin{pmatrix} u_{n\uparrow} \\ v_{n\downarrow} \end{pmatrix} \tag{C.1}$$

and

$$\begin{pmatrix} \hat{h_\downarrow} & \Delta_i \\ \Delta_i^* & -\hat{h_\uparrow}^* \end{pmatrix} \begin{pmatrix} u_{n\downarrow} \\ v_{n\uparrow} \end{pmatrix} = E_{n\downarrow} \begin{pmatrix} u_{n\downarrow} \\ v_{n\uparrow} \end{pmatrix} \tag{C.2}$$

We will now show that it suffices to solve one of the eqs. C.1 and C.2 in order to obtain all information about the system. If $\begin{pmatrix} u_{n\uparrow} \\ v_{n\downarrow} \end{pmatrix}$ is an eigenvector in eq. C.1 with a negative eigenvalue $-E_{n\uparrow}$ we have (suppressing the spin indices):

$$\begin{aligned} &\begin{pmatrix} \hat{h} & -\Delta_i \\ -\Delta_i^* & -\hat{h}^* \end{pmatrix} \begin{pmatrix} u_n \\ v_n \end{pmatrix} = -E_n \begin{pmatrix} u_n \\ v_n \end{pmatrix} \\ \implies &\begin{pmatrix} -\hat{h} & \Delta_i \\ \Delta_i^* & \hat{h}^* \end{pmatrix} \begin{pmatrix} u_n \\ v_n \end{pmatrix} = E_n \begin{pmatrix} u_n \\ v_n \end{pmatrix} \\ \implies &\begin{pmatrix} -\hat{h}^* & \Delta_i^* \\ \Delta_i & \hat{h} \end{pmatrix} \begin{pmatrix} u_n^* \\ v_n^* \end{pmatrix} = E_n \begin{pmatrix} u_n^* \\ v_n^* \end{pmatrix} \\ \implies &\begin{pmatrix} \hat{h} & \Delta_i \\ \Delta_i^* & -\hat{h}^* \end{pmatrix} \begin{pmatrix} v_n^* \\ u_n^* \end{pmatrix} = E_n \begin{pmatrix} v_n^* \\ u_n^* \end{pmatrix}. \end{aligned} \tag{C.3}$$

Hence, if $\begin{pmatrix} u_{n\uparrow} \\ v_{n\downarrow} \end{pmatrix}$ is an eigenvector of the matrix in eq. C.1 with a negative eigenvalue $-E_{n\uparrow}$, $\begin{pmatrix} v_{n\uparrow}^* \\ u_{n\downarrow}^* \end{pmatrix}$ is an eigenvector of the matrix in eq. C.2 with a positive eigenvalue $E_{n\downarrow}$. So in the numerical calculations, we only need to solve eq. C.2.

Appendix D: Density of particles

Along with the superconducting order parameter another self-consistent field is the density of electrons. The density is affected by for instance the presence of impurities on certain sites. The average density on a site i is given by the expectation value of the number operator.

$$\langle \hat{n}_i \rangle = \langle c_{i\uparrow}^\dagger c_{i\uparrow} \rangle + \langle c_{i\downarrow}^\dagger c_{i\downarrow} \rangle. \tag{D.1}$$

By plugging in thetransformation in eq. 2.23 this becomes:

$$\langle \hat{n}_i \rangle = \sum_n \langle (u^*_{n,i\uparrow}\gamma^\dagger_{n\uparrow} - v_{n,i\uparrow}\gamma_{n\downarrow})(u_{n,i\uparrow}\gamma_{n\uparrow} + v^*_{n,i\uparrow}\gamma^\dagger_{n\downarrow})\rangle \tag{D.2}$$

$$+ \sum_n \langle (u^*_{n,i\downarrow}\gamma^\dagger_{n\downarrow} + v_{n,i\downarrow}\gamma_{n\uparrow})(u_{n,i\downarrow}\gamma_{n\downarrow} + v^*_{n,i\downarrow}\gamma^\dagger_{n\uparrow})\rangle \tag{D.3}$$

$$= \sum_n \langle |u_{n,i\uparrow}|^2\gamma^\dagger_{n\uparrow}\gamma_{n\uparrow} + |v_{n,i\uparrow}|^2\gamma_{n\downarrow}\gamma^\dagger_{n\downarrow} + u^*_{n,i\downarrow}v^*_{n,i\downarrow}\gamma^\dagger_{n\uparrow}\gamma^\dagger_{n\downarrow} + u_{n,i\uparrow}v_{n,i\uparrow}\gamma_{n\downarrow}\gamma_{n\uparrow}\rangle \tag{D.4}$$

$$+ \sum_n \langle |u_{n,i\downarrow}|^2\gamma^\dagger_{n\downarrow}\gamma_{n\downarrow} + |v_{n,i\downarrow}|^2\gamma_{n\uparrow}\gamma^\dagger_{n\uparrow} + u^*_{n,i\downarrow}v^*_{n,i\downarrow}\gamma^\dagger_{n\downarrow}\gamma^\dagger_{n\uparrow} + u_{n,i\downarrow}v_{n,i\downarrow}\gamma_{n\uparrow}\gamma_{n\downarrow}\rangle. \tag{D.5}$$

Using that $\langle \gamma^\dagger_{n\sigma}\gamma_{n'\sigma'}\rangle = f(E_{n\sigma})\delta_{nn'}\delta_{\sigma\sigma'}$ and $\langle \gamma_{n\sigma}\gamma_{n'\sigma'}\rangle = 0$ we obtain

$$\langle \hat{n}_i \rangle = \sum_n \left[|u_{n,i\uparrow}|^2 f(E_{n\uparrow}) + |v_{n,i\uparrow}|^2(1 - f(E_{n\downarrow})) + |u_{n,i\downarrow}|^2 f(E_{n\downarrow}) + |v_{n,i\downarrow}|(1 - f(E_{n\uparrow})) \right]. \tag{D.6}$$

The sum is over the n's which correspond to positive eigenvalues E_n. Using the correspondence between positive and negative eigenvalues found in appendix C, the sum can be rewritten to a sum over all eigenvalues, both positive and negative. We also use that $1 - f(E) = f(-E)$. We then get the final expression for the electron density:

$$\langle \hat{n}_i \rangle = \sum_k |u_{l,i\uparrow}|^2 f(E_{l\uparrow}) + |v_{l,i\downarrow}|^2(1 - f(E_{l\uparrow})), \tag{D.7}$$

which in the case of no spin dependence reduces to:

$$\langle \hat{n}_i \rangle = \sum_l \left[|u_{l,i}|^2 f(E_l) + |v_{l,i}|^2(1 - f(E_l)) \right]. \tag{D.8}$$

Appendix E: Peierls substitution

In this section some intermediate steps, which we need to perform in order to obtain the Peierls phases are presented. First, we will consider the expression:

$$\begin{aligned} (\mathbf{p} + e\mathbf{A})a(\mathbf{r} - \mathbf{R}_i)e^{-i\frac{e}{\hbar}\Lambda_i} &= e\mathbf{A}a(\mathbf{r} - \mathbf{R}_i)e^{-i\frac{e}{\hbar}\Lambda_i} + e^{-i\frac{e}{\hbar}\Lambda_i}\mathbf{p}a(\mathbf{r} - \mathbf{R}_i) + a(\mathbf{r} - \mathbf{R}_i)\left(-e\nabla\Lambda_i\right) \\ &= e^{-i\frac{e}{\hbar}\Lambda_i}(\mathbf{p} - e\nabla\Lambda_i + e\mathbf{A})a(\mathbf{r} - \mathbf{R_i}) \\ \implies (\mathbf{p} + e\mathbf{A})^2 a(\mathbf{r} - \mathbf{R}_i)e^{-i\frac{e}{\hbar}\Lambda_i} &= e^{-i\frac{e}{\hbar}\Lambda_i}(\mathbf{p} - e\nabla\Lambda_i + e\mathbf{A})^2 a(\mathbf{r} - \mathbf{R}_i). \end{aligned} \tag{E.1}$$

We perform integration by parts on the following integral:

$$\begin{aligned} \int_0^1 \mathbf{A}(\mathbf{R}_i + \lambda(\mathbf{r} - \mathbf{R}_i))d\lambda &= \Big[\lambda\mathbf{A}(\mathbf{R_i} + \lambda(\mathbf{r} - \mathbf{R_i}))\Big]_0^1 - \int_0^1 d\lambda\, \lambda \frac{d\mathbf{A}(\mathbf{R}_i + \lambda(\mathbf{r} - \mathbf{R}_i))}{d\lambda} \\ &= \mathbf{A}(\mathbf{r}) - \lambda\int_0^1 d\lambda\, \frac{d\mathbf{A}}{d\mathbf{r}'}\frac{d\mathbf{r}'}{d\lambda} = \mathbf{A}(\mathbf{r}) - \int_0^1 d\lambda\, \left((\mathbf{r} - \mathbf{R}_i)\cdot\nabla\right)\mathbf{A}. \end{aligned} \tag{E.2}$$

Using the identities $\nabla \times \mathbf{r} = 0$ and $(\mathbf{A}\cdot\nabla)\mathbf{r} = \mathbf{A}$ as well as the fact that

$$\nabla \times \mathbf{A}(\mathbf{R}_i + \lambda(\mathbf{r} - \mathbf{R}_i)) = \lambda\mathbf{B}(\mathbf{R}_i + \lambda(\mathbf{r} - \mathbf{R}_i)),$$

we are now ready to calculate (using the generator Λ_i in eq. 3.7):

$$\begin{aligned}\nabla\Lambda_i &= \int_0^1 d\lambda\Big[\left((\mathbf{r}-\mathbf{R}_i)\cdot\nabla\right)\mathbf{A} + (\mathbf{A}\cdot\nabla)\cdot(\mathbf{r}-\mathbf{R}_i) + (\mathbf{r}-\mathbf{R_i})\times(\nabla\times\mathbf{A}) + \mathbf{A}\times\nabla\times(\mathbf{r}-\mathbf{R}_i)\Big] \\ &= \mathbf{A}(\mathbf{r}) + \int_0^1 d\lambda\Big[-\mathbf{A}(\mathbf{R}_i+\lambda(\mathbf{r}-\mathbf{R}_i)) + \mathbf{A}(\mathbf{R}_i+\lambda(\mathbf{r}-\mathbf{R}_i)) + (\mathbf{r}-\mathbf{R}_i)\times(\lambda\mathbf{B})(\mathbf{R_i}+\lambda(\mathbf{r}-\mathbf{R}_i))\Big] \\ &= \mathbf{A}(\mathbf{r}) + \int_0^1 d\lambda\lambda(\mathbf{r}-\mathbf{R}_i)\times\mathbf{B}(\mathbf{R_i}+\lambda(\mathbf{r}-\mathbf{R}_i)).\end{aligned} \tag{E.3}$$

Plugging the field operators in eq. 3.6 into the Hamiltonian in eq. 3.1 and using eqs. E.3 and we obtain:

$$\begin{aligned}H &= \int d\mathbf{r}\sum_{i\sigma} a^*(\mathbf{r}-\mathbf{R}_i)e^{i\frac{e}{\hbar}\Lambda_i}c^\dagger_{i\sigma}\Big[\frac{1}{2m}\left(\frac{\hbar}{i}\nabla_{\mathbf{r}}+e\mathbf{A}(\mathbf{r})\right)+V(\mathbf{r})-E_F\Big]\sum_{j\sigma}a(\mathbf{r}-\mathbf{R}_j)e^{-i\frac{e}{\hbar}\Lambda_j}c_{j\sigma} \\ &= \sum_{ij\sigma}\tilde{h}_{ij}c^\dagger_{i\sigma}c_{j\sigma},\end{aligned} \tag{E.4}$$

where

$$\begin{aligned}\tilde{h}_{ij} = \int d\mathbf{r}a^*(\mathbf{r}-\mathbf{R_i})e^{i\frac{e}{\hbar}(\Lambda_i-\Lambda_j)}\Bigg[&\frac{1}{2m}\big(\mathbf{p}-e\int_0^1 d\lambda\lambda(\mathbf{r}-\mathbf{R_j})\times\mathbf{B}(\mathbf{R_j}+\lambda(\mathbf{r}-\mathbf{R_j}))\big)^2 \\ &+V(\mathbf{r})-E_F\Bigg]a(\mathbf{r}-\mathbf{R_j}),\end{aligned} \tag{E.5}$$

is the single-particle Hamiltonian in the presence of a magnetic field. Hence, we are able to express the Hamiltonian on the usual tight-binding form, even though the single-particle Hamiltonian now contains some complicated terms arising from the gauge transformation.

Appendix F: Magnetic translation operators

Requiring that:

$$\left[T_x^M, T_y^M\right] = 0 \tag{F.1}$$

$$\left[T_i^M, H\right] = 0, \tag{F.2}$$

we can derive the equations which fix the phases $\theta^x_{m,n}$ and $\theta^y_{m,n}$

$$\left[T_x^M, T_x\right] = e^{i\theta^x_{m+1,n}}e^{i\phi^x_{m,n}} - e^{i\phi^x_{m+1,n}}e^{i\theta^x_{m,n}} \stackrel{!}{=} 0. \tag{F.3}$$

The discrete lattice derivative is defined according to:

$$\Delta_x f_{m,n} = f_{m+1,n} - f_{m,n} \tag{F.4}$$

$$\Delta_y f_{m,n} = f_{m,n+1} - f_{m,n}. \tag{F.5}$$

From eq. F.3 we get the relation

$$\begin{aligned}\phi^x_{m+1,n} - \phi_{m,n} &= \theta_{m+1,n} - \theta^x_{m,n} \\ &\implies \Delta_x\phi^x_{m,n} = \Delta_x\theta^x_{m,n}.\end{aligned} \tag{F.6}$$

Furthermore:

$$\begin{aligned}\left[T_x^M, T_y\right] &= e^{i\theta^x_{m,n+1}} e^{i\phi^y_{m,n}} - e^{i\phi^y_{m+1,n}} e^{i\theta^x_{m,n}} \stackrel{!}{=} 0 \\ &\implies \Delta_x \phi^y_{m,n} = \Delta_y \theta^x_{m,n} \\ &\implies \Delta_x \phi^y_{m,n} = \Delta_y \phi^x_{m,n} + 2\pi\Phi_{m,n}.\end{aligned} \tag{F.7}$$

We also have:

$$\begin{aligned}\left[T_y^M, T_x\right] &= e^{i\theta^y_{m+1,n}} e^{i\phi^x_{m,n}} - e^{i\phi^x_{m,n+1}} e^{i\theta^y_{m,n}} \stackrel{!}{=} 0 \\ &\implies \Delta_y \phi^x_{m,n} = \Delta_x \theta^y_{m,n} \\ &\implies \Delta_y \phi^x_{m,n} = \Delta_x \phi^y_{m,n} - 2\pi\Phi_{m,n}.\end{aligned} \tag{F.8}$$

Finally,

$$\begin{aligned}\left[T_y^M, T_y\right] &= e^{i\theta^y_{m,n+1}} e^{i\phi^y_{m,n}} - e^{i\phi^y_{m,n+1}} e^{i\theta^y_{m,n}} \stackrel{!}{=} 0 \\ &\implies \Delta_y \phi^y_{m,n} = \Delta_y \theta^y_{m,n}.\end{aligned} \tag{F.9}$$

The equations F.6, F.7, F.8 and F.9 are solved by the phases:

$$\theta^x_{m,n} = \phi^x_{m,n} + 2\pi\Phi_{m,n} n \tag{F.10}$$

$$\theta^y_{m,n} = \phi^y_{m,n} - 2\pi\Phi_{m,n} m. \tag{F.11}$$

Appendix G: Supercurrents

From the continuity equation we have:

$$\left(\nabla \cdot \hat{\mathbf{j}}\right)_i = -\frac{\partial \hat{\rho}_i}{\partial t} = e\dot{\hat{n}}_i = \frac{ie}{\hbar} \sum_{j\sigma} \left(t_{ji} e^{i\phi_{ji}} c^\dagger_{j\sigma} c_{i\sigma} - t_{ij} e^{i\phi_{ij}} c^\dagger_{i\sigma} c_{j\sigma} \right). \tag{G.1}$$

The total current between sites i and j is determined by considering one term j and plugging in the transformation in eq. 2.23

$$\begin{aligned}\langle j_{i\to j} \rangle &= \frac{ie}{\hbar} \Big[t_{ji} e^{i\phi_{ji}} \langle c^\dagger_{j\uparrow} c_{i\uparrow} \rangle - t_{ij} e^{i\phi_{ij}} \langle c^\dagger_{i\uparrow} c_{j\uparrow} \rangle + t_{ji} e^{i\phi_{ji}} \langle c^\dagger_{j\downarrow} c_{i\downarrow} \rangle - t_{ij} e^{i\phi_{ij}} \langle c^\dagger_{i\downarrow} c_{j\downarrow} \rangle \Big] \\ &= \frac{ie}{\hbar} \Big[t_{ji} e^{i\phi_{ji}} \Big\langle \Big(\sum_n u^*_{n,j\uparrow} \gamma^\dagger_{n\uparrow} + v_{n,j\uparrow} \gamma_{n\downarrow} \Big) \Big(\sum_n u_{n,i\uparrow} \gamma_{n\uparrow} + v^*_{n,i\uparrow} \gamma^\dagger_{n\downarrow} \Big) \Big\rangle \\ &- t_{ij} e^{i\phi_{ij}} \Big\langle \Big(\sum_n u^*_{n,i\uparrow} \gamma^\dagger_{n\uparrow} + v_{n,i\uparrow} \gamma_{n\downarrow} \Big) \Big(\sum_n u_{n,j\uparrow} \gamma_{n\uparrow} + v^*_{n,j\uparrow} \gamma^\dagger_{n\downarrow} \Big) \Big\rangle \\ &+ t_{ji} e^{i\phi_{ji}} \Big\langle \Big(\sum_n u^*_{n,j\downarrow} \gamma^\dagger_{n\downarrow} + v_{n,j\downarrow} \gamma_{n\uparrow} \Big) \Big(\sum_n u_{n,i\downarrow} \gamma_{n\downarrow} + v^*_{n,j\downarrow} \gamma^\dagger_{n\uparrow} \Big) \Big\rangle \\ &- t_{ij} e^{i\phi_{ij}} \Big\langle \Big(\sum_n u^*_{n,i\downarrow} \gamma^\dagger_{n\downarrow} + v_{n,i\downarrow} \gamma_{n\uparrow} \Big) \Big(\sum_n u_{n,j\downarrow} \gamma_{n\downarrow} + v^*_{n,j\downarrow} \gamma^\dagger_{n\uparrow} \Big) \Big\rangle.\end{aligned} \tag{G.2}$$

By expanding the parentheses and using that since the Bogoliubon operators represent fermions $\langle \gamma^\dagger_{n\sigma}\gamma_{n'\sigma'}\rangle = f(E_k)\delta_{nn'}\delta_{\sigma\sigma'}$ and $\langle \gamma_{n\sigma}\gamma_{n'\sigma'}\rangle = 0$, we get that:

$$\begin{aligned}\langle j_{i\to j}\rangle = \frac{ie}{\hbar}\sum_n \Big[& t_{ji}e^{i\phi_{ji}}(u^*_{n,j\uparrow}u_{n,i\uparrow}f(E_{n\uparrow}) + v_{n,j\uparrow}v^*_{n,i\uparrow}f(-E_{n\downarrow})) \\ & - t_{ij}e^{i\phi_{ij}}(u^*_{n,i\uparrow}u_{n,j\uparrow}f(E_{n\uparrow}) + v_{n,i\uparrow}v^*_{n,j\uparrow}f(-E_{n\downarrow})) \\ & + t_{ji}e^{i\phi_{ji}}(u^*_{n,j\downarrow}u_{n,i\downarrow}f(E_{n\downarrow}) + v^*_{n,i\downarrow}v_{n,j\downarrow}f(-E_{n\uparrow})) \\ & - t_{ij}e^{i\phi_{ij}}(u^*_{n,i\downarrow}u_{n,j\downarrow}f(E_{n\downarrow}) + v^*_{n,j\downarrow}v_{n,i\downarrow}f(-E_{n\uparrow}))\Big].\end{aligned} \tag{G.3}$$

All the preceding sums over n are over positive eigenvalues only. We can rewrite this by exploiting that a positive eigenvalue $E_{n\downarrow}$ with eigenvector $\begin{pmatrix} v^*_{n\uparrow} \\ u^*_{n\downarrow}\end{pmatrix}$ corresponds to a negative eigenvalue $-E_{n\uparrow}$ with eigenvector $\begin{pmatrix} u_{n\uparrow} \\ v_{n\downarrow}\end{pmatrix}$, so

$$\begin{aligned}\langle j_{i\to j}\rangle = \frac{ie}{\hbar} & \sum_{n,E_n>0} t_{ji}e^{i\phi_{ji}}u^*_{n,j\uparrow}u_{n,i\uparrow}f(E_{n\uparrow}) + \sum_{n,E_n<0} t_{ji}e^{i\phi_{ji}}u^*_{n,j\uparrow}u_{n,i\uparrow}f(E_{n\uparrow}) \\ & - \sum_{n,E_n>0} t_{ij}e^{i\phi_{ij}}u^*_{n,i\uparrow}u_{n,j\uparrow}f(E_{n\uparrow})) - \sum_{n,E_n<0} t_{ij}e^{i\phi_{ij}}u^*_{n,i\uparrow}u_{n,j\uparrow}f(E_{n\uparrow}) \\ & + \sum_{n,E_n<0} t_{ji}e^{i\phi_{ji}}v^*_{n,i\downarrow}v_{n,j\downarrow}f(-E_{n\uparrow}) + \sum_{n,E_n>0} t_{ji}e^{i\phi_{ji}}v^*_{n,i\downarrow}v_{n,j\downarrow}f(-E_{n\uparrow}) \\ & - \sum_{n,E_n<0} t_{ij}e^{i\phi_{ij}}v^*_{n,j\downarrow}v_{n,i\downarrow}f(-E_{n\uparrow}) - \sum_{n,E_n>0} t_{ij}e^{i\phi_{ij}}v^*_{n,j\downarrow}v_{n,i\downarrow}f(-E_{n\uparrow}) \\ = \frac{ie}{\hbar} & \sum_l \left[t_{ji}e^{i\phi_{ji}}u^*_{l,j\uparrow}u_{l,i\uparrow} - t_{ij}e^{i\phi_{ij}}u^*_{l,i\uparrow}u_{l,j\uparrow}\right] f(E_{l\uparrow}) \\ & + \sum_l \left[t_{ji}e^{i\phi_{ji}}v^*_{l,i\downarrow}v_{l,j\downarrow} - t_{ij}e^{i\phi_{ij}}v_{l,i\downarrow}v^*_{l,j\downarrow}\right] f(-E_{l\uparrow}).\end{aligned} \tag{G.4}$$

Appendix H: Impurities

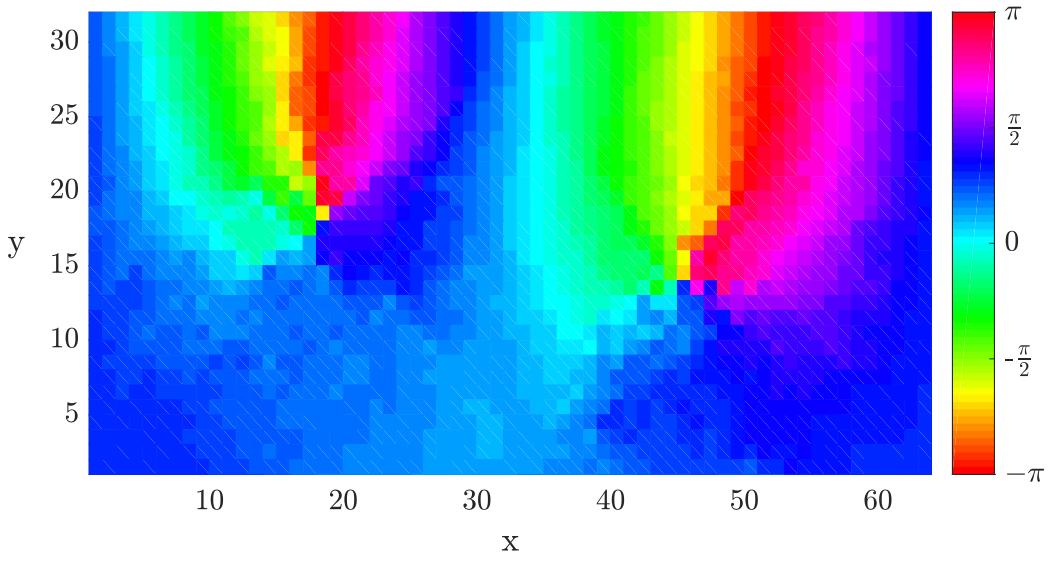

(a)

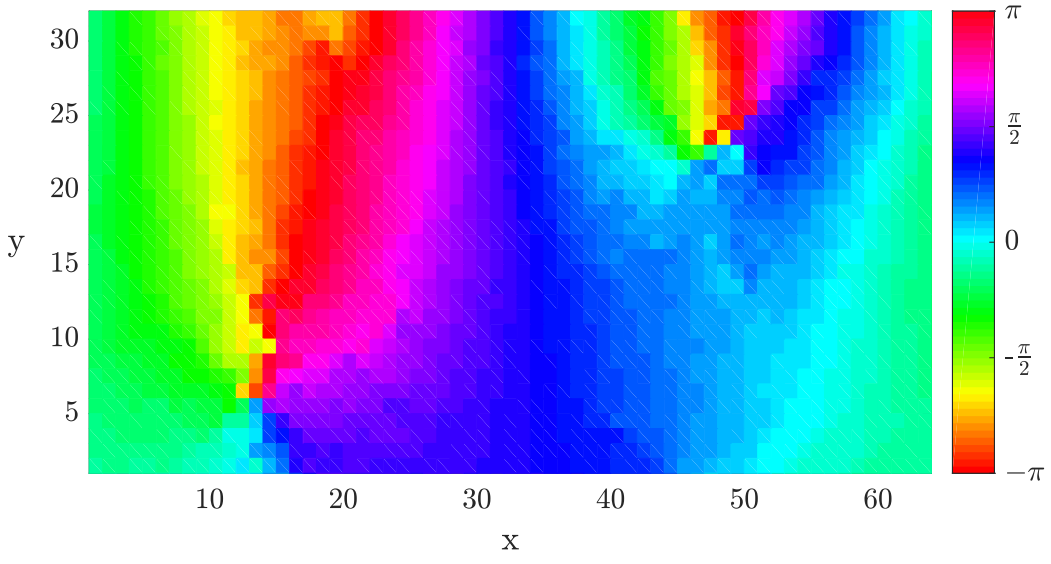

(b)

Figure H.1.: Complex phase of the SCOP at $k_BT = 0.02$ (a) and $k_BT = 0.07$ (b), that is below and above the critical temperature for the homogeneous system respectively. In both cases summing the phases differences along a closed path around the borders of each square half of the system yields the value -2π. This confirms that vortices are present in both cases

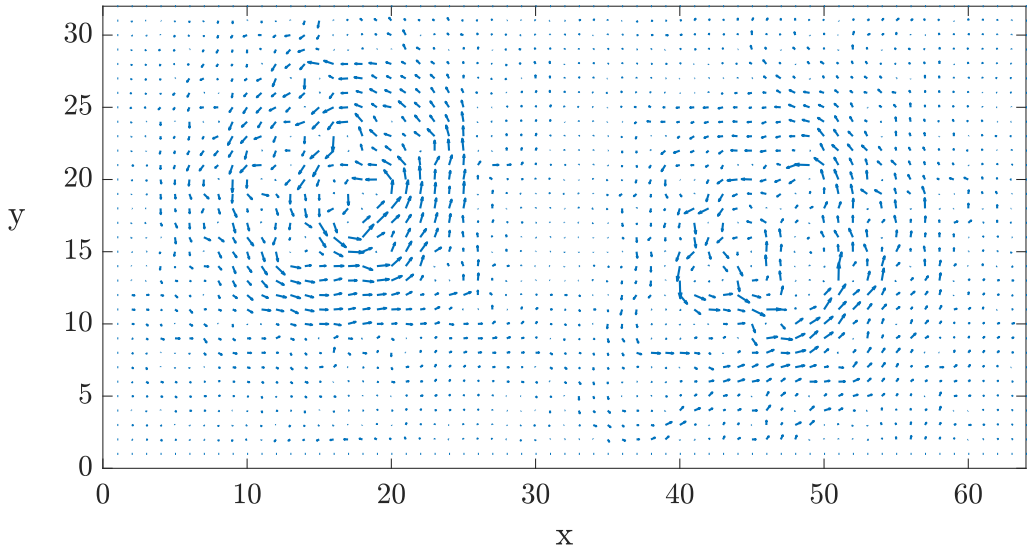

(a)

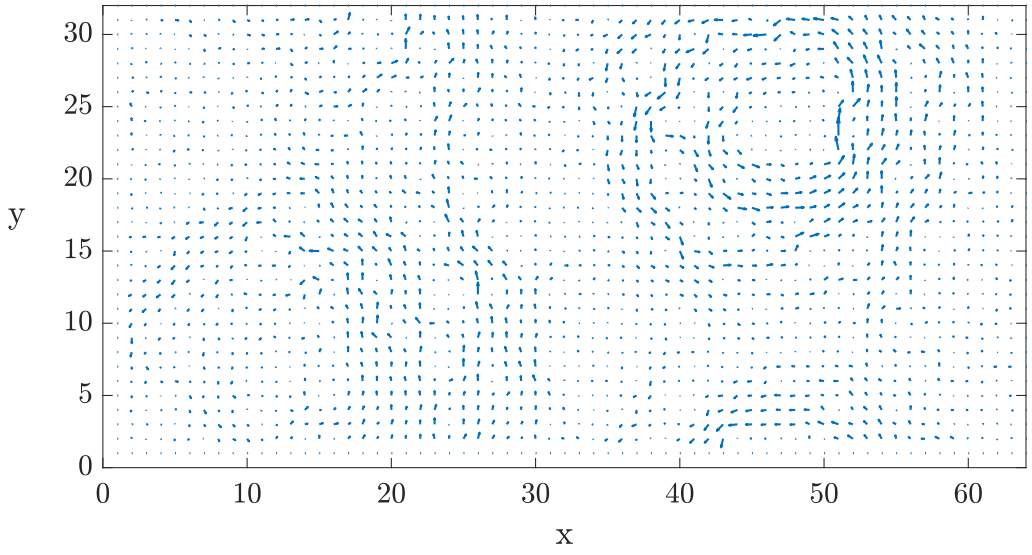

(b)

Figure H.2.: Supercurrents in a system with parameters $t = 1$, $t' = -0.2$ and $V = -1.5t$, and repulsive impurities of strength $V^{imp} = 10t$ randomly distributed on 15 % of the lattice sites. a) is $k_B T = 0.02$, that is below T_c for the system without impurities, and the supercurrents are easily seen to be circulating the vortices. b) shows $k_B T = 0.07$, and thus we are above T_c for the homogeneous system. However, vortices are still present and circulated by the currents, even though the magnitude of the currents vectors is smaller than in a).

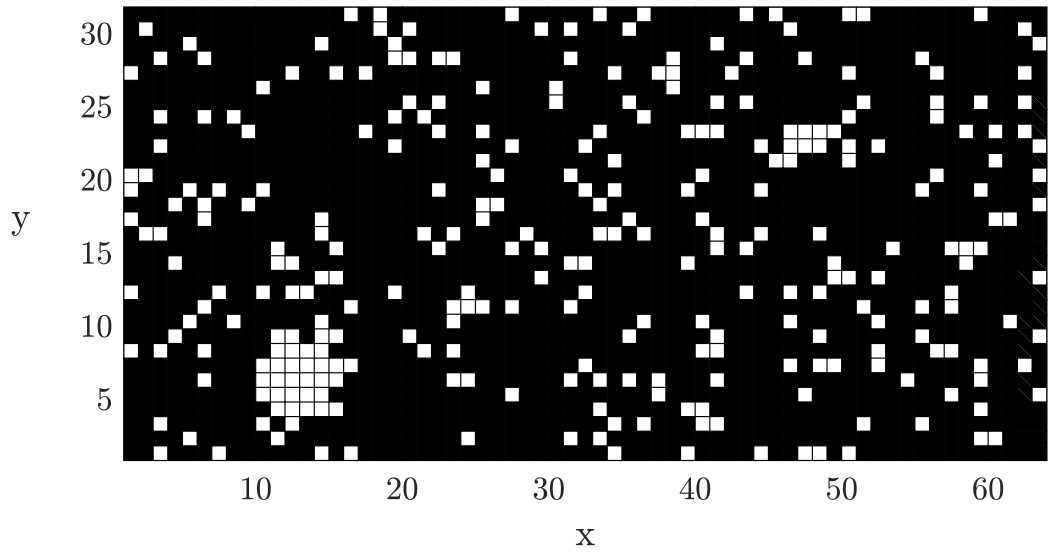

(a)

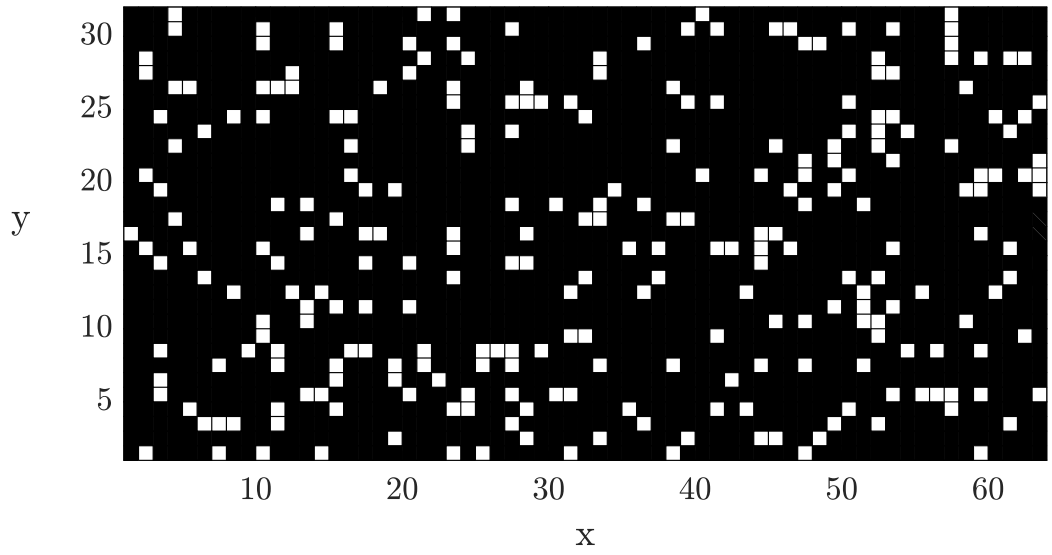

(b)

Figure H.3.: Plot showing whether the magnitude of the SCOP on each lattice site is either $|\Delta_i| < p\Delta_0$ (white) or $|\Delta_i| > p\Delta_0$ (black) for $p = 0.1$. $k_B T = 0.07$ for both (a) and (b). All edges are connected by paths of black points in both plots. This is also the case for all $p \leq 0.4$ with a magnetic field and with $p \leq 0.45$ for $B = 0$. Hence we are at $T < T_c$ according to the definition of T_c used by Gastiasoro and Andersen [1].